CHARLES UNIVERSITY

Faculty of Science

Study programme: Biology

Study field: Parasitology

Bc. Barbora Šmídová

The role of nitric oxide in mice infected with *Trichobilharzia regenti*, the neuropathogenic schistosome

Úloha oxidu dusnatého při nákaze myší neuropatogenní schistosomou *Trichobilharzia regenti*

MASTER'S THESIS

Supervisor: Mgr. Tomáš Macháček

Prague 2019

PROHLÁŠENÍ

Prohlašuji, že jsem závěrečnou práci zpracovala samostatně a že jsem uvedla všechny použité informační zdroje a literaturu. Tato práce ani její podstatná část nebyla předložena k získání jiného nebo stejného akademického titulu.

V Praze dne 12. 8. 2019

……

Bc. Barbora Šmídová

ACKNOWLEDGEMENTS

My warmest gratitude and greatest thanks go to my supervisor Tomáš Macháček for all his guidance, help and patience throughout my master's studies.

Thanks also belong to Martin Majer and Jana Bulantová for their introduction to methods essential for completing my experiments; to Irena Parohová for her help and extra set of hands during the experiments; to Ondřej Šebesta and Miroslav Hyliš for their help with advanced microscopy; to Martin Schätz for his help with image analysis; to Tatiana Spitzová for her help with statistics; and to the rest of our lab for creating a friendly environment.

I'm also grateful to Líba, Dáďa and Víťa who have patiently listened to all my problems and cheered me up and to Dan for the hours of talks over the litres of coffee. Lastly, I'd like to express my thanks to my family for their financial and emotional support during my studies.

Experimental work performed within this thesis was funded by Charles University Grant Agency (project no. 729516) and Czech Science Foundation (18-11140S).

ABSTRACT

Nitric oxide (NO) has been proved to reduce parasite burden in vertebrates infected with *Schistosoma*, *Fasciola*, *Brugia* or *Taenia*. NO negatively influences parasite growth and development, which then leads to smaller parasite-caused damage to the liver during schistosomosis and stimulates healing processes in muscles infected with *Toxocara canis*. Peroxynitrite, formed from NO and superoxide, significantly reduces the viability of *F. hepatica* adults. In case of *T. regenti*, the neuropathogenic schistosome, the cells capable of NO production (macrophages, neutrophils, eosinophils, microglia and astrocytes) migrate to the site of the infection suggesting that NO might affect *T. regenti* infection as well. Therefore, the production of NO and its effect on the course of the infection was examined *in vivo* and the effect of peroxynitrite on *T. regenti* schistosomula was examined *in vitro* to assess the role of reactive nitrogen species during the infection. Our results from *in vivo* experiments demonstrate that although the infection did not significantly elevate nitrite/nitrate results in the sera, NO is locally produced in the early stages of the infection in both the skin and the spinal cord as shown by immunohistochemical detection of inducible NO synthase. Diminishing NO production by aminoguanidine treatment did not reveal any significant effect of NO neither on worm burden nor nervous tissue pathology, particularly demyelination. I*n vitro* experiments revealed that peroxynitrite significantly reduced schistosomula viability and severely damaged the integrity of tegument and mitochondria, which was assessed by measurement of lactate production and electron microscopy, respectively. Based on our results, we hypothesize that NO influences *T. regenti* infection in mice only in the early stages later leaving the parasite clearance to other immune effectors, possibly Th2 related. Taken together, this thesis has made a step in recognizing the effector molecules of *T. regenti* clearance in mice.

Keywords: nitric oxide; *Trichobilharzia regenti*; skin; spinal cord; inducible NO synthase; 3-nitrotyrosine; aminoguanidine; peroxynitrite

ABSTRAKT

Oxid dusnatý (NO) je jednou z efektorových molekul zodpovědných za snížení počtu parazitů v případě nákazy obratlovců helminty rodů *Schistosoma*, *Fasciola*, *Brugia* nebo *Taenia*. NO zpomaluje růst a vývoj lidských schistosom, což v důsledku vede k mírnější patologii jater. V případě nákazy škrkavkou *Toxocara canis* NO stimuluje opravu poškozené svalové tkáně. NO může mimo jiné reagovat se superoxidem za vzniku peroxynitritu, který prokazatelně snižuje viabilitu dospělců rodu *Fasciola hepatica*. Migrace imunitních buněk, které jsou schopny produkovat NO (jmenovitě makrofágy, neutrofily, eozinofily, mikroglie a astrocyty) do místa infekce byla popsána i při nákaze myší neuropatogenní schistosomou *Trichobilharzia regenti*. To napovídá tomu, že by NO mohl ovlivňovat i průběh infekce touto schistosomou. Proto se *in vivo* část tato práce věnuje výzkumu produkce NO v důsledku infekce a jeho efekt na samotný průběh infekce, zatímco *in vitro* část zkoumá vliv peroxynitritu na samotná schistosomula. Výsledky *in vivo* části ukazují, že infekce *T. regenti* sice signifikantně nezvýšila množství nitritů a nitrátů v séru, ale v rané fázi infekce stimulovala lokální produkci NO v nakažené kůži a míše. Snížení produkce NO podáváním aminoguanidinu nicméně výrazně neovlivnilo počet nalezených červů ani množství myelinu v míše. V *in vitro* experimentech bylo prokázáno, že peroxynitrit výrazně snížil životaschopnost schistosomul a vážně poškodil jejich tegument a mitochondrie. Výsledky naznačují, že NO nebo peroxynitrit ovlivňuje infekci myší *T. regenti* pouze v rané fázi a pak přenechává místo jiným molekulám, které by mohly být spojené s Th2 imunitní odpovědí. Experimenty v rámci této práce pomohly s odhalováním molekul zodpovědných za eliminaci nákazy myší *T. regenti.*

Keywords: oxid dusnatý; *Trichobilharzia regenti*; kůže; mícha; inducibilní NO syntáza; 3-nitrotyrosin; aminoguanidin; peroxynitrit

List of contents

Abbreviations

1400W	N-[[3-(aminomethyl)phenyl]methyl]-ethanimidamide
3-NT	3-nitrotyrosine
AG	aminoguanidine
Arg-1	arginase
BME	Basal Medium Eagle
BSA	bovine serum albumin
cNOS	constitutive NO synthase
CNS	central nervous systém
D.E.R. 736	diglycidyl ether of polypropylene glycol
DAPI	4’,6-diamidine-2’-phenylindole
DEA/NO	diethylamine NONOate
DETA/NO	diethylentriamin/NO
DMAE	dimethylaminoethanol
dpi	days post infection
EM	electron microscopy
eNOS	endothelial NO synthase
ESP	excretory-secretory products
GFAP	glial fibrillary acidic protein
hpi	hours post infection
i.p.	intraperitoneally
Iba-1	ionized calcium-binding adaptor molecule
IFN-γ	interferon gamma
IHC	immunohistochemistry, immunohistochemical
IL	interleukin
iNOS	inducible NO synthase
iNOS-/-	iNOS KO
$iNOS^{+/-}$	iNOS heterozygote
KO	knocked-out
L-NAME	N^G-nitro-L-arginin metyl ester
L-NIL	NG-(1-iminoethyl)-lysine
L-NMMA	N^G-monometyl-L-arginin
LPS	lipopolysaccharide
MAF	macrophage activating factors

MBP	myelin basic protein
nNOS	neuronal NO synthase
NO	nitric oxide
NSA	nonenyl succinic anhydride
p.o.	perorally
PAMPs	pathogen-associated molecular patterns
PBS	phosphate-buffered saline
PSCs	protoscoleces
PZQ	praziquantel
RNS	reactive nitrogen species
ROS	reactive oxygen species
SCM	schistosomula cultivation medium
SEM	scanning electron microscopy
SIN-1	5-amino-3-(4-morpholinyl)-1,2,3-oxadiazolium chloride
SNAP	S-nitroso-N-acetyl-DL-penicillamine
TEM	transmission electron microscopy
TNF-α	tumor necrosis factor alpha
wpi	weeks post infection
WT	wild type

1. Introduction and aims of the study

The production of nitric oxide (NO) in response to the infection has been described in cases of *Schistosoma*, *Fasciola*, *Echinococcus*, *Brugia* and other helminths or even unicellular pathogens. For example, during schistosomosis, NO has been proved to increase parasite clearance and slow down parasite development and maturation, which indirectly protects liver from severe damage (Shen et al., 2017). In case of *Trichobilharzia regenti*, the neuropathogenic schistosome, mice can eliminate the infection, probably thanks to effective immune response. Nevertheless, the molecule with such effect during the infection has not been identified yet.

Therefore, this thesis is focused on examining the NO production in mice infected with *T. regenti*, the role of NO during the infection and the effect of peroxynitrite, a toxic reactive nitrogen species (RNS), on parasite itself to enable better understanding of parasite elimination in resistant mammals.

The aims of the thesis were to:

- Analyze systemic nitric oxide production during infection by measurement of nitrite/nitrate levels.
- Detect iNOS (the source of NO) and 3-nitrotyrosine (3-NT) (the marker of a nitrosative stress) in affected skin and spinal cord.
- Examine the changes in parasite burden and amount of myelin basic protein (MBP) after administration of iNOS inhibitor.
- Determine the effect of peroxynitrite on schistosomula *in vitro* with focus on their viability and ultrastructure pathology.

2. Literature review

2.1. NO as a part of an immune system

NO is a gaseous molecule produced both in vertebrates and invertebrates playing an important role in cell signaling or immune response. The enzyme responsible for production of NO used for the cell signaling is called constitutive nitric oxide synthase (cNOS). It is found in neurons (nNOS) or endothelial cells (eNOS) and is synthesized at all times.

On the other hand, inducible NOS (iNOS) is responsible for NO production in response to pathogens or tissue damage. Major iNOS expressing cells are neutrophils (Garcia-Bonilla et al., 2014), macrophages (Stuehr et al., 1989) or eosinophils (Paoliello-Paschoalato et al., 2005) and also keratinocytes (Sirsjö et al., 1996), hepatocytes (Curran et al., 1989) or endothelial cells (Oswald et al., 1994). iNOS synthesis begins after the cell recognizes an activating molecule formerly known as macrophage activation factor (MAF) (Bogdan, 2001), pathogen-associated molecular pattern (PAMP), such as lipopolysaccharide (LPS) (Stuehr and Marletta, 1985) or parasitic antigens such as schistosome glycans (Thomas et al., 2003) and *Leishmania* proteophosphoglycan (Samant et al., 2009). After the cells are activated by these factors and/or cytokines such as interferon γ (IFN-γ), tumor necrosis factor α (TNF-α) or interleukin 2 (IL-2) (James, 1995), iNOS is expressed and arginine is used as a substrate for NO production (Bogdan, 2001).

NO is very reactive and is considered a radical. It can bind with O_2 and form nitrites and nitrates (Beckman and Koppenol, 1996). These molecules are stable and can be detected in the blood sera, plasma or urine obtained from infected animals (Asensio et al., 1993; Greenberg et al., 1995; Rabelo et al., 2016; Ruano et al., 2012). NO can also react with superoxide and form more reactive, aggressive and stable peroxynitrite (Beckman and Koppenol, 1996; Huie and Padmaja, 1993).

NO and peroxynitrite, collectively called RNS, protect the organism by affecting many parasitic cell structures, such as proteins (Bogdan et al., 2000), nucleic acids (Beckman et al., 1992; Juedes and Wogan, 1996) and lipids in the membrane (Fang, 1997). It can also damage or inactivate enzymes important for proper cell function. For example, peroxynitrite was proven to damage mitochondria by binding to the Fe-S center of aconitase (Hausladen and Fridovich, 1994) and by cytochrome p450 inactivation (Vernia et al., 2001). NO can bind to hem centers in enzymes, such as mitochondrial cytochrome c oxidase (Wade and Castro, 1990), which leads to increased reactive oxygen species (ROS) levels. This can result in formation of more peroxynitrite and more severe cellular damage (Cleeter et al., 1994) (for summary see Figure 1).

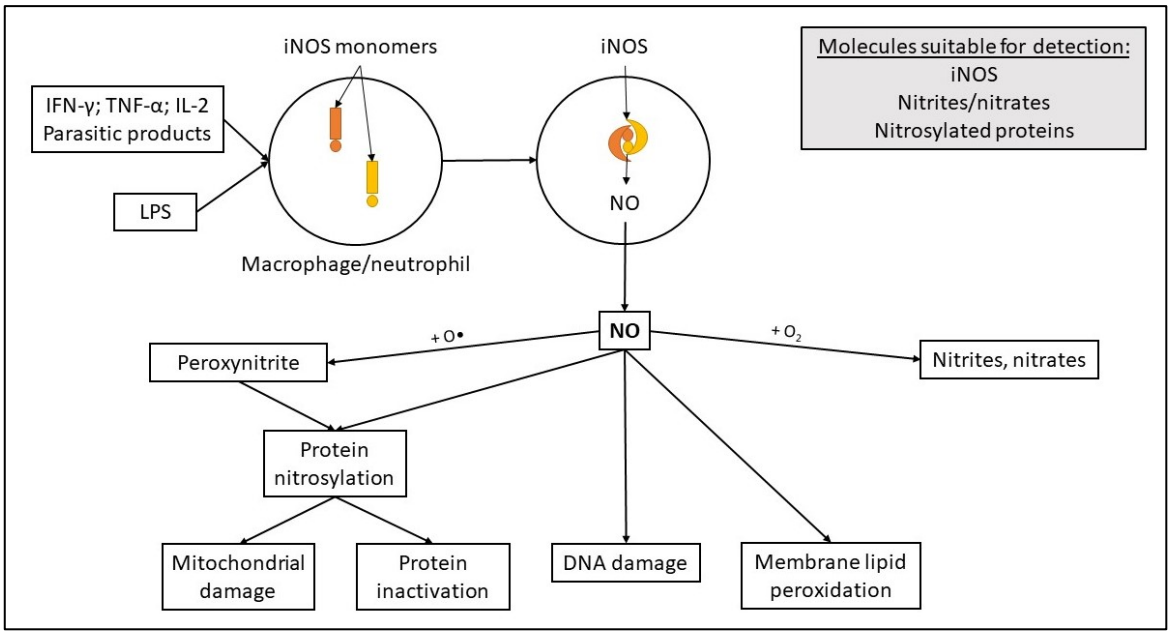

Figure 1: Summary of NO production and effects. After an immune cell (macrophage or neutrophil) recognizes activating molecules (IFN-γ, TNF-α, IL-2 or LPS), iNOS monomers are synthesized and form an active dimer to produce NO. This can then react with O_2 to form nitrites or nitrates or with O• to form peroxynitrite, which can then impair mitochondrial function. NO can alter protein structure by nitrosylation, damage DNA or react with lipids in the membrane. Nitrites, nitrates, iNOS and nitrosylated proteins can be used for indirect NO detection in the organism.

The role of NO in parasitic infections can be studied *in vitro* and *in vivo*. As for the first, NO or ONOO- donors, such as LA419 (Ruano et al., 2015), DETA/NO (diethylentriamin/NO) (Ahmed et al., 1997; Ruano et al., 2012) and SIN-1 (5-amino-3-(4-morpholinyl)-1,2,3-oxadiazolium chloride) (Hahn et al., 2001; Ruano et al., 2012) are used to test direct effects of RNS on parasites. A different *in vitro* approach studies competitive iNOS inhibitors like L-NMMA (N^G-monometyl-L-arginin) (Coulson et al., 1998; Gray and Lawrence, 2002; Ruano et al., 2012) or L-NAME (N^G-nitro-L-arginin metyl ester) (Andrade et al., 2007; Ruano et al., 2012) in cell cultures producing NO to verify the contribution of iNOS.

More complex interactions can be studied in infected experimental animals, where it is also possible to influence NO production. iNOS inhibitors can be used in these *in vivo* experiments as well and can be administered to the experimental animals either intraperitoneally (i.p.) or perorally (p.o.). Aminoguanidine (AG) is commonly used (Brunet et al., 1999; Demirci et al., 2006; Espinoza et al., 2002; Gargili et al., 2004; Gupta et al., 2004; Kołodziej-Sobocińska et al., 2006; Wynn et al., 1994) but also L-NMMA (Coulson et al., 1998; Gray and Lawrence, 2002), L-NAME or N^G-(1-iminoethyl)-lysine (L-NIL) (Hirata et al., 2001) can be applied. Moreover, experimental animals with knocked-out (KO) genes are used for more accurate NO production impairment. It is possible to use

iNOS KO animals (Shen et al., 2017), which provides most specific and accurate results for research of NO effects. Alternatively, mice KO in genes modifying immune response in general, such as STAT4 (Rodríguez-Sosa et al., 2004) or STAT6 (Alonso-Trujillo et al., 2007) that impairs Th2 or Th1 immune response, respectively, can be used. However, this leads to complex alteration of the immune response and it is usually hard to assess the particular role of iNOS in such experiments.

Each of these methods has both its advantages and disadvantages. Generally speaking, well defined *in vitro* systems are easier to use and are focused on the effect of one or few particular molecules. Therefore, they provide only partial insight. On the other hand, using *in vivo* systems provides more complex insight but tend to be focused on host pathology, not the effect of NO on the parasite itself. For the best evidence of NO effects during infections it is best to combine both approaches.

2.2. NO effects on helminths and in helminthiases

Due to its reactivity, NO plays an important role in fight against infectious agents. NO can affect both parasite and host well-being and the effect is usually stage- and host-dependent. Although its effects are best known in infections caused by protists like *Toxoplasma*, *Leishmania*, *Plasmodium* or *Trypanosoma* (Brunet, 2001), in this thesis NO effects in helminth infections of vertebrates are discussed. This subchapter offers summary of various NO effects on helminths and on vertebrate hosts during helminthiases sorted by parasite relevance to the topic of the thesis and amount of knowledge on NO effects.

2.2.1. *Schistosoma* sp. and schistosomosis

Schistosoma sp. is a blood-dwelling parasite and it is the causative agent of human schistosomosis. The larval stages called cercariae emerge from freshwater snails and penetrate the skin of submerged body parts of swimmers or workers. After penetration, cercariae transform into schistosomula, migrate through the blood system to their final location and mature. Adults then produce eggs that can get through bloodstream into organs like liver, bladder or, rarely, brain and stimulate pathological granuloma formation here.

In 1980s, several authors have reported that activated macrophages efficiently killed *S. mansoni* schistosomula *in vitro* (Krammer et al., 1985; McLaren and James, 1985; Sher et al., 1982). McLaren and James (1985) observed quick and permanent attachment of the peritoneal macrophages onto the surface of *in vitro* transformed schistosomula. Intact tegument but clearly damaged muscles were noticed after 4-hour incubation. It was later proved that IFN-γ was one of the MAFs important for successful schistosomula killing (Esparza et al., 1987) and that NO produced by activated macrophages cultured with schistosomula damages and kills the parasites (James and Glaven,

1989). It was also postulated that NO inhibits respiratory chain of the parasite which ultimately leads to their death (James and Glaven, 1989).

Further *in vitro* experiments suggest that, after the skin penetration, newly transformed schistosomula are susceptible to activated macrophages (Sher et al., 1982). Then, during the vascular migration, schistosomula might be prone to NO produced by activated endothelial cells (Oswald et al., 1994). Nevertheless, as schistosomula migrate to the lungs, their metabolism is no more aerobic and schistosomula are resistant to NO effects until they get to liver and again rely on aerobic metabolism (Ahmed et al., 1997). The results support the hypothesis stated above that NO negatively affects schistosomula mitochondria.

Unlike *in vitro* experiments, which are mostly focused on NO effects on schistosomula viability, *in vivo* experiments are often focused on parasite-induced host pathology. When AG was administered to infected mice, more necrotic loci were observed in the liver when compared with liver from non-treated infected mice (Brunet et al., 1999). The importance of NO production for liver protection was also described using $iNOS^{-/-}$ and WT mice as $iNOS^{-/-}$ mice could not down-regulate the egg-induced inflammation and granuloma formation as well as WT mice (Hesse et al., 2000). The NO production by iNOS depends on arginine which is also a substrate for arginase (Arg-1). Arg-1 is associated with Th2 response and if it takes all the substrate, it can tilt the immune response further towards Th2 and prevent NO from protecting the liver. Analysis of iNOS and Arg-1 mRNA from infected murine liver showed that impairing Th2 response led to higher levels of NO and milder pathology in the liver (Hesse et al., 2001) proving protective NO effect during liver stage of schistosomosis.

Sometimes even a small change in the protocol can lead to opposite results of the experiments. Such was the case of research done by Wynn et al. (1994) and Coulson et al. (1998). Both teams immunized their mice by irradiated cercariae, infected them with cercariae and measured iNOS levels in the lungs. So far, their results agree – immunization led to higher iNOS and NO levels and smaller parasite burden. Both teams wanted to confirm the NO role by administration of different iNOS inhibitors to mice. Wynn et al. used AG, while Coulson et al. used L-NMMA. Although both inhibitors are substrate-competitive, L-NMMA is more specific, whereas AG influences other NO synthases as well (Nilsson, 1999). Adding AG led to higher parasite burden which led the authors to the conclusion that NO is protective during this infection (Wynn et al., 1994). L-NMMA didn't have same effect as AG, though. Due to this, Coulson et al. claimed that mere inhibition of NO production doesn't properly indicate NO role and that other immune effectors are probably important during the infection. To prove their hypothesis, they repeated the experiment with $iNOS^{-/-}$ and $iNOS^{+/-}$

mice. Immunization led to smaller number of surviving parasites in both groups but the differences were statistically insignificant. In their eyes, this confirmed their previous hypothesis and they claim that immunization is helpful albeit not by strengthening NO production like Wynn et al. thought but rather by supporting trapping mechanisms in the lungs (Coulson et al., 1998). Nevertheless, Coulson et al. used iNOS$^{-/-}$ mice with imperfect gene knock-out and it's possible that some level of iNOS was produced even in this group. To decide whether the truth lies with Wynn et al. (1994) or Coulson et al. (1998), it would be necessary to perform the experiment once again, this time with properly knocked-out iNOS gene.

Besides *S. mansoni*, also *S. japonicum* is used as a model in experiments. For establishing the role of NO role, two iNOS inhibitors – L-NIL or L-NAME, were administered to infected mice. Although NO inhibition led to higher number of granulomas, less immune cells infiltrated the granuloma site and pathology was milder. It seems that NO protects liver from severe damage both in *S. mansoni* and *S. japonicum* infections (Hirata et al., 2001).

A crucial role of NO in control of *S. japonicum* infection was recently demonstrated in rats naturally resistant to the infection. First observation showed that rats produced more NO and killed more parasites than susceptible mice or iNOS$^{-/-}$ rats. Moreover, parasites obtained from WT rats were smaller, thinner, less developed and produced non-viable eggs. Liver granulomas in WT rats were significantly smaller and less dense compared to iNOS$^{-/-}$ rats (Figure 2). On the other hand, granuloma formation after injecting viable eggs was independent on NO production, which is in accordance with results published by Hesse et al. (2000). Altogether these results suggest that NO production is important for slowing down schistosome growth and development and it indirectly reduces granuloma size by disabling egg development in adult females (Shen et al., 2017).

Lately, resistance to praziquantel (PZQ), usually very effective treatment of schistosomosis, appeared. Associating PZQ with furoxans, NO donors, luckily revealed several drug candidates effective both in inactivating recombinant thioredoxin glutathione reductase, which is important for ROS neutralization in parasitic cells, and in killing adult schistosomes. These drug candidates could be used in areas where schistosomes are resistant to PZQ itself as they employ both PZQ and NO effects on the parasites (Guglielmo et al., 2014).

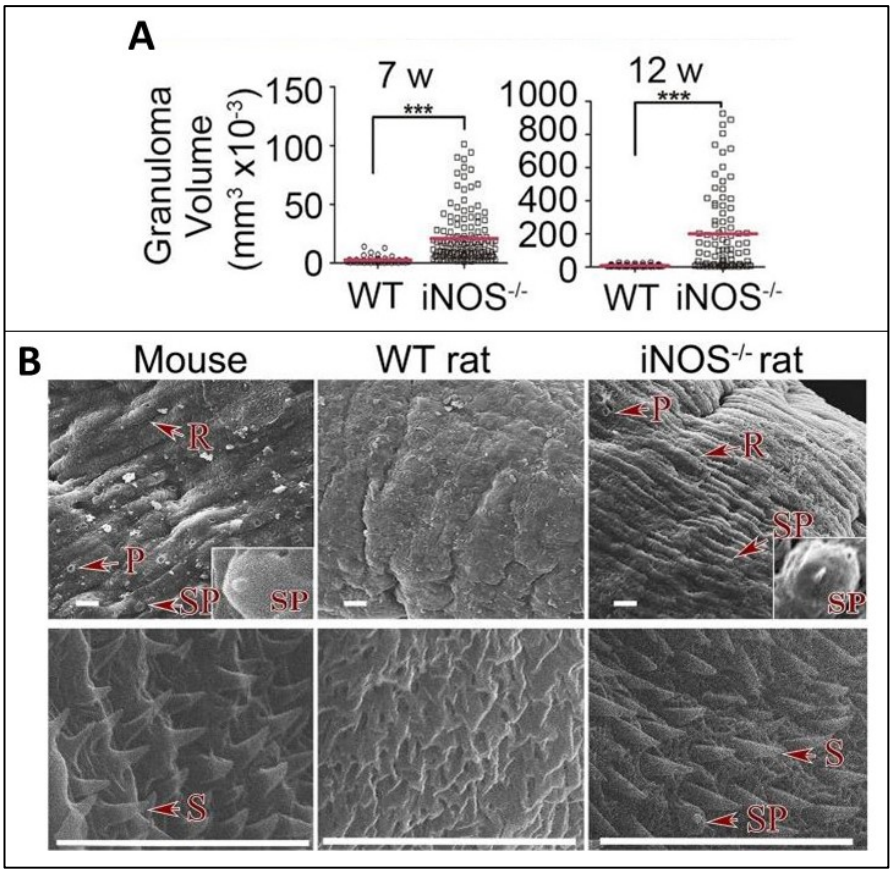

Figure 2: Differences in liver granuloma volume in WT and iNOS$^{-/-}$ rats infected with S. mansoni (A) and differences in tegumental structure in parasites obtained from these rats and infected mice (B), adapted from Shen et al. (2017). A: *Inhibition of NO production led to bigger liver granulomas both 7 and 12 weeks post infection pointing to the protective role of NO in schistosoma-induced liver pathology*. B: *Adult* S. mansoni *tegument analysis using scanning electron microscopy both on body (upper line of images) and oral sucker (lower line of images).* Scale bars = 10 µm. Tegument of parasites obtained from WT rats producing more NO than mice and iNOS$^{-/-}$ rats is smoother compared to tegument of parasites obtained from the other 2 groups. Abbreviations: R – ridge, P – pit, S – spine, SP – sensory papillae.

2.2.2. *Fasciola hepatica* and fasciolosis

Fasciola hepatica cercariae develop in snails, leave them and form resistant metacercariae on vegetation. These are infectious for the definitive hosts, cattle and sheep, in which the flukes mature in liver and dwell in bile ducts. When other animals, such as rats, are infected by this fluke, their immune system manages to eliminate the infection before the flukes reach adulthood (Hayes and Mitrovič, 1977).

The difference in susceptibility with respect to NO was tested on cells isolated from sheep and rats, susceptible and resistant hosts, respectively. Rat peritoneal cells stimulated with LPS or blood serum from infected rats attached to the juvenile flukes, produced NO and killed the juveniles.

Adding L-NMMA to the culture reversed the effect and more fluked survived, which pointed directly to effect of NO. Ovine cells were not able to produce NO and/or kill the parasites after adding any of tested stimulants (Piedrafita et al., 2001). Their results suggest that the difference in host susceptibility is caused by different NO production after infection with this fluke.

The rat ability to kill juvenile flukes by NO production mainly in the early stage of infection was confirmed by an *in vitro* and an *in vivo* study performed on peritoneal cells. First, peritoneal cells obtained 4 and 7 days post infection (dpi) were cultivated with *F. hepatica* excretory-secretory products (ESP) or juveniles. Moreover, juveniles were cultivated with NO donor S-nitroso-N-acetyl-DL-penicillamine (SNAP). The results showed that juveniles stimulated higher NO production than ESP, but mere NO could not kill as many flukes as immune cells. This means that even though NO could be protective during the infection, more than just NO production is necessary for host protection Sibille et al. (2004). Later, peritoneal cells were examined further and apparently, NO is produced first by eosinophils, later by macrophages and neutrophils and at 4 dpi NO is replaced by other radicals, mostly ROS (Jedlina et al., 2011). It is therefore possible that considering the effect of ROS, peroxynitrite might be relevant here.

The effect of the afore-mentioned peroxynitrite was explored on adults cultivated in bile. Peroxynitrite was added to one half of the cultures. When comparing the two tested groups, they found out that peroxynitrite is indeed capable of killing adults (Sadeghi-Hashjin and Naem, 2001). Although these results support the above-mentioned theory, more experiments would be required to confirm that peroxynitrite is the molecule responsible for killing *F. hepatica*.

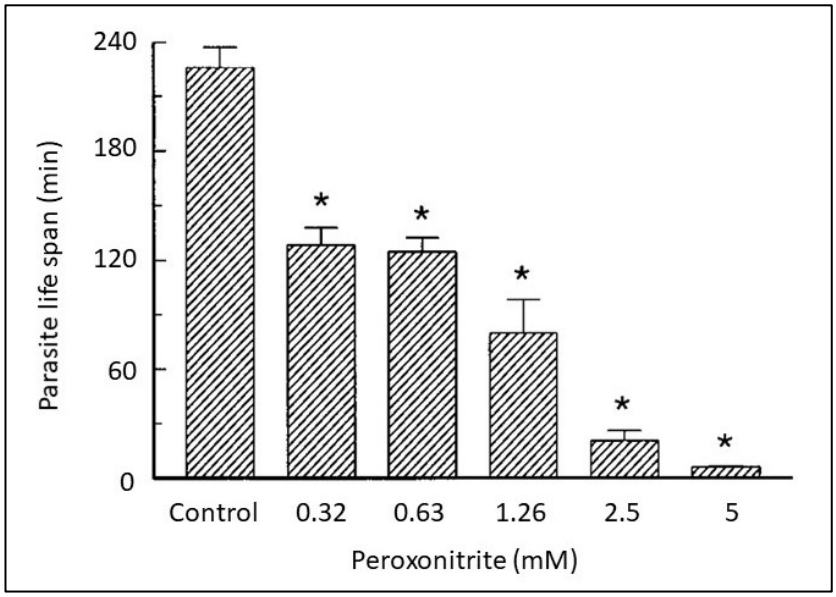

Figure 3: The effect of peroxynitrite on cultivated F. hepatica *adults*, adapted from Sadeghi-Hashjin and Naem (2001). Peroxynitrite increased parasite mortality (immobile parasite were considered dead) in a concentration-dependent manner.

Due to the facts that *F. hepatica* stimulates NO production and that RNS kill juvenile flukes, the effect of immunization on the course of infection was examined. Immunization by *F. hepatica* cathepsin L1 led to stronger iNOS production in the goat liver (Zafra et al., 2013) and higher NO levels produced by sheep peritoneal cells (Pérez-Caballero et al., 2018). Along with that, smaller liver lesions in the infected goats (Zafra et al., 2013) and up to 9 dpi even in sheep were observed in immunized animals (Pacheco et al., 2017). Similar results were obtained from infected mice immunized by synthetic peptides containing T-cell epitopes. Immunized mice were more efficient in parasite eradication and their liver was less damaged when compared to non-immunized mice. Taken together, results from goats (Zafra et al., 2013), sheep (Pacheco et al., 2017; Pérez-Caballero et al., 2018) and mice (Rojas-Caraballo et al., 2017) point to a possible use of NO supporting vaccines in liver protection during *F. hepatica* infection.

2.2.3. *Echinococcus* sp. and echinococcosis

Echinococcus sp. is a tapeworm with two-host cycle, in which even humans can be recognized as intermediate hosts. They get infected by ingesting tapeworm eggs from which larvae called hexacanths are released in the intestine. Hexacanths then migrate to inner organs or muscles, transform into larvae called metacestodes and form two-layered cysts. Metacestodes are the pathogenic agent in human echinococcosis and are often studied due to that.

The first step in recognizing the NO role was done in a simple experiment where *E. multilocularis* protoscoleces (PSCs) were cultivated with macrophages. Macrophages were stimulated by IFN-γ with or without LPS and the best ability to kill PSCs was shown by macrophages stimulated with both IFN-γ and LPS. Enzymes deactivating ROS and iNOS inhibitor L-NMMA were used to rule out the protective role of ROS and to ascribe the effect directly to NO, respectively. On one hand, adding ROS deactivating enzymes did not affect PSCs killing, on the other, adding L-NMMA led to higher survival rate of PSCs (Kanazawa et al., 1993).

Similar experiment was performed on PSCs isolated from pulmonary hydatids cultivated with peripheral blood mononuclear cells obtained from echinococcosis patients and the results are consistent with the previous findings – L-NMMA reversed deadly NO effects on PSCs. In this experiment, the PSCs effect on NO production was also examined. Apparently, PSCs stimulate production of NO, the molecule efficient in killing them (Amri et al., 2007). On the other hand, PSCs are rarely in contact with the peripheral blood cells, usually only when the cyst breaks and then the NO stimulation is useful for host protection.

Although the effect on PSCs has been described, NO would have to damage the cyst wall to reach them. After *E. granulosus* cysts were cultivated with activated macrophages or NO donor SNAP, cyst structure analysis showed that NO presence causes separation of laminar and germinal layer and subsequently cyst death. The researchers performing this experiment also claimed that it is possible that laminar layer of viable cyst is not a mere mechanical barrier protecting the parasite but that it also influences the NO production (Steers et al., 2001). It was later proved that the laminar layer negatively affects the NO production (Amri and Touil-Boukoffa, 2015), unlike PSCs, suggesting its role in protection of inner germinal layer. Besides laminated layer, parasite-derived miR-71 and other molecules included in *E. multilocularis* extracellular vesicles can also downregulate NO production (Zheng et al., 2016, 2017). However, their real contribution to downregulation of host immune response needs to be confirmed.

Contrary to *in vitro* data, long-term (4 months) infections of WT C57BL/6 and iNOS$^{-/-}$ mice with *E. multilocularis* show slightly different trends. Metacestodes grew and proliferated more in WT mice than in iNOS$^{-/-}$ mice. Moreover, splenocytes obtained from infected WT animals stimulated by *E. multilocularis* somatic antigen, concanavalin A and LPS show low T-cell proliferation and higher NO production when compared to iNOS$^{-/-}$ splenocytes (Dai et al., 2003). This suggests that NO dysregulates T-cell proliferation, therefore negatively influences effective immune response to echinococcus infection (Dai and Gottstein, 1999; Dai et al., 2004).

Similarly to fasciolosis, the role of NO was also examined by comparison of susceptible (BALB/c mice) and resistant (C57BL/6J mice) hosts. Macrophages obtained from C57BL/6 mice in the early stage of *E. granulosus* infection (1 – 7 dpi) produced more NO and killed more PSCs than those from infected BALB/c mice (Mourglia-Ettlin et al., 2015). It is therefore possible that NO production in the early stages of echinococcosis, when the parasite migrates to its final localization, is important for the host protection, while in the later infection NO supports metacestodes growth by disrupting T-cell proliferation (Dai et al., 2003), as suggested by Zheng (2013).

2.2.4. *Brugia malayi* and filariosis

During mosquito blood feeding, *Brugia malayi* L3 larvae migrate through proboscis to their definite hosts – humans. Here they travel to lymph nodes, mature, mate and produce larvae called microfilariae. These then circulate through blood stream and mosquitoes then suck them while feeding.

In 1996, Taylor et al. (1996) cultivated *Brugia malayi* microfilaria with NO donor SNAP and observed lower motility in microfilariae. Adding L-NMMA to the culture reversed the negative effect on parasite motility. The basis of the effect is unclear, though, as L-NMMA is a competitive inhibitor of

iNOS and has nothing known to do with NO donors. Thomas et al. (1997) then moved further and tested the NO effects on both microfilariae and adults. Instead of SNAP, SIN-1 was used. This donor generates both NO and ROS that form peroxynitrite. Peroxynitrite immobilized even more microfilariae than mere NO but had no effect on adults. Brugia could therefore be one of the helminths affected by peroxynitrite rather than by NO. Different susceptibility of the stages is in accordance with general idea that microfilariae need oxidative metabolism for their movement (Rew and Saz, 1977) which, in this case, was disabled by RNS. The results are similar to schistosomes, where NO affects mitochondrial respiration in younger schistosomula with oxidative metabolism.

The effect of NO donor, DEA/NO, was also tested *in vivo* and was compared to AG effects. Administration of AG increased parasite burden in mice contrary to DEA/NO, which significantly reduced parasite number at 5 wpi. Moreover, administering DEA/NO to mice in chronic stage of the infection reduced parasite motility. Similarly, treating L3 larvae with DEA/NO *in vitro* led to temporary and reversible paralysis of the larvae (Rajan et al., 1996). This shows that even though NO affects parasite motility, it is not sufficient for parasite killing.

Another approach was tested using resistant (Natal multimammate mice) and susceptible (gerbils) hosts. In gerbils live and developing larvae and macrophages capable of attachment to larvae but not producing enough NO were observed. On the other hand, in multimammate mice the parasite burden was lower and NO levels were higher leading to parasite elimination. AG treatment of multimammate mice increased the number of live larvae but the number was still smaller than the number of surviving larvae in gerbils. The conclusion is that NO cannot be the sole factor protecting the host (Gupta et al., 2004). It is possible that NO only immobilizes the worms (Rajan et al., 1996) but peroxynitrite kills them, which would support the hypothesis made based on *in vitro* results.

As for the vaccines related to increment of NO production, Verma et al. (2015) tried to find the candidates in adult filariae homogenate. They have chosen three fractions proven to stimulate NO production and used them for rat immunization. After filarial infection they measured NO levels produced by splenocytes and counted the microfilariae. One fraction appeared to be very protective and stimulating NO production, therefore this was chosen for testing its effects after adding AG. AG treatment caused a drop in NO levels and a rise in larval numbers. This research confirms the protective role of NO and suggests a candidate vaccine for filariases.

2.2.5. *Trichinella spiralis* and trichinellosis

Trichinella spiralis can be found only inside of its numerous hosts, it is never in the environment. There are two phases of trichinellosis – intestinal and muscular. During the intestinal phase, when

the parasite stimulates iNOS synthesis in the intestinal epithelial cells (Ming et al., 2016), higher nitrite levels correlate with worse pathology in murine intestines (Hadas et al., 2001; Lawrence et al., 2000). Administration of AG to infected mice improved gut health but supported parasite survival in mice (Kołodziej-Sobocińska et al., 2006). Taken together, these results show that NO is responsible for intestinal damage during first stage of trichinellosis.

Too strong inflammation is usually harmful to the parasite and *Trichinella spiralis* was proved to down-regulate iNOS production as soon as 3 dpi both in intestine and in other organs such as lungs or spleen (Bian et al., 2001). The authors hypothesize that suppressing NO production on the system level might facilitate larval migration which would lead to higher parasite burden, similarly to filarias.

In muscles, larvae stimulate "nurse cell" formation and immune cells infiltrate the surroundings. When eosinophils were depleted (PHIL mice) and absent in the infiltrate around nurse cells, it led to poorly regulated Th1 response and lower parasite burden and elevated IFN-γ and nitrite levels in cervical lymph nodes cell cultures. Histological analysis revealed iNOS present around the damaged nurse cells in PHIL mice (Figure 4). The results suggest that NO is effective in killing the larvae inside the nurse cells (Fabre et al., 2009). Nevertheless, it can also harm the host in the process, therefore the host regulates this by eosinophils, although they save a part of the larvae.

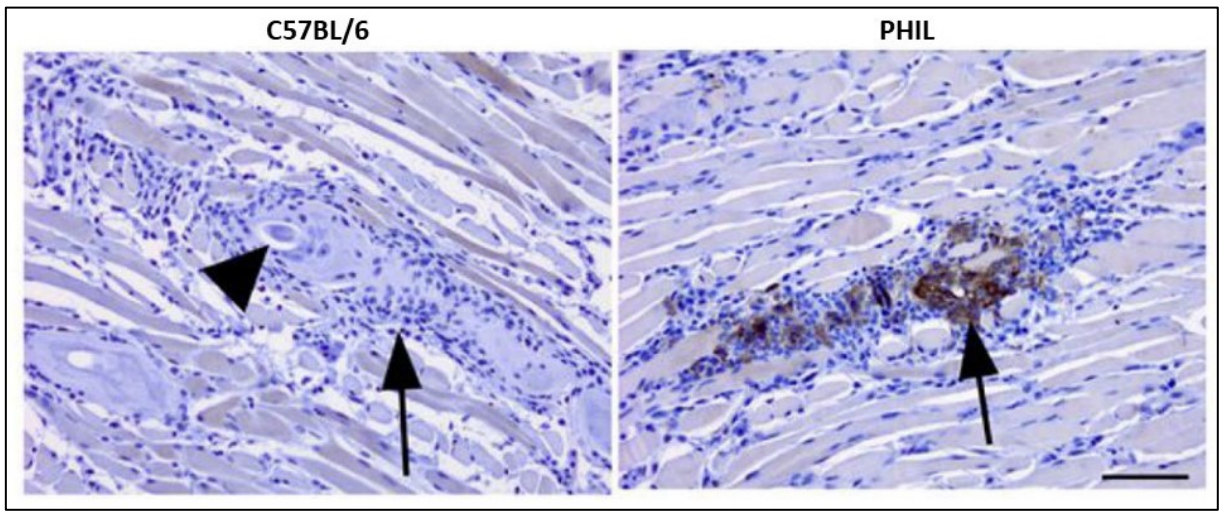

Figure 4: Detection of iNOS (brown) in skeletal muscle of C57BL/6 and PHIL mice infected with T. spiralis, *adapted from* Fabre et al. (2009). Arrowhead indicates larva and arrows indicate cellular infiltrates. Scale bar = 100 µm. Eosinophil depletion (PHIL mice) led to elevated IFN-γ and nitrite levels in infected animals resulting in smaller parasite burden.

2.2.6. Other helminths and helminthoses

Taenia crassiceps has a similar development as *Echinococcus* sp. and its cysticerci can cause human cysticercosis. Two approaches were applied to indirectly test the NO effects during cysticercosis: one employing STAT4$^{-/-}$ mice, another using STAT6$^{-/-}$ mice. STAT4 is a transcription factor important for Th1 response, which has been proved to be protective in this infection (Terrazas et al., 1999). The knock-out of STAT4 resulted in higher number of surviving cysticerci, lower splenocyte proliferation and lower levels NO and TNF-α in activated macrophages when compared to WT mice infections (Rodríguez-Sosa et al., 2004). On the other hand, STAT6 is important for Th2 response and less parasites survived in STAT6$^{-/-}$ mice when compared with WT mice. Administration of the NO inhibitor L-NAME to infected mice increased parasite survival in both tested groups, confirming the protective role of NO (Alonso-Trujillo et al., 2007). Although all these results show that NO could be host-protective during cysticercosis, more experiments, preferably on iNOS$^{-/-}$ mice, need to be performed.

Strongyloides venezuelensis is a nematode with infective L3 stage and percutaneous or peroral route of infection. After somatic migration larvae mature and mate in the intestine. Study focused on L3 larvae and adults revealed that DETA/NO immobilizes rather larvae than adults but significantly affects both stages (Ruano et al., 2012). This difference might be due to different metabolisms of the stages as was the case with *Brugia malayi* and schistosomes. NO effects were also examined *in vivo* first in mice treated by AG or LA419, NO donor, later in WT and iNOS$^{-/-}$. In all tested groups iNOS/NO levels negatively correlated with parasite load (Rodrigues et al., 2018; Ruano et al., 2015). When mice immunocompromised by dexamethasone were treated by AG or LA419, similar trends were observed (Ruano et al., 2015). Therefore, NO is noticeably protective in this infection as it immobilized infective larvae and protected both immunocompetent and immunocompromised hosts.

Toxocara canis larvae are the causative agent of human toxocarosis. There is an evidence that iNOS and IFN-γ mRNA expression rose in the CNS after infection in both susceptible BALB/c mice and resistant NIH mice (Hamilton et al., 2008) suggesting that NO might have some effect during toxocarosis. Indeed, L-NIL treatment prior to infection increased the diameter of muscle granulomas and reduced collagen deposition (Lin et al., 2008). Given that collagen formation is a part of the healing process, the results suggest that NO protects the host tissue during toxocarosis, similarly to schistosomosis. Similarly, AG treatment of rats two days prior to the infection worsened pulmonary damage when compared to non-treated infected group (Espinoza et al., 2002) supporting the protective effect of NO. Two more studies focused on the effects of AG on

experimental toxocarosis were carried out and both examined the damage caused to the organs (Demirci et al., 2006; Gargili et al., 2004). They examined lungs, liver and brain of infected mice, AG was given to half of them and reported less sever organ damage in AG-treated animals, opposite to the results by Espinoza et al. (2002). However, there are several flaws in the studies, such as mentioning non-existing enzyme called lipid peroxidase, using badly chosen markers for oxidative stress etc., therefore the results need to be assessed and interpreted cautiously.

This literature review shows that NO has multiple effects during helminthiases and only a few of them have been studied in enough detail. NO can affect parasite's motility and mortality or host pathology. There is no one "generally correct" answer to the question: What is the role of NO during helminthoses? There are more answers to this question depending on the species, even stage of the parasite and they can also differ between host species. The main effects related to the infection of the vertebrate hosts are summarized in Table 1.

Table 1: Summary of RNS effects during selected helminthoses

Parasite	Effect of RNS on the parasite			Effect of NO on host pathology	References
	development	motility	viability		
Schistosoma sp.	NO impaired adult development and egg production (*in vivo*)	N/A	NO killed liver schistosomula (*in vitro*)	Positive: smaller granuloma, milder liver damage	Ahmed et al., 1997; Brunet et al., 1999; Hesse et al., 2001; James and Glaven, 1989; Krammer et al., 1985; McLaren and James, 1985; Shen et al., 2017; Sher et al., 1982
Fasciola hepatica	N/A	Peroxynitrite immobilized adults	peroxynitrite killed adults, NO killed juveniles (*in vitro*)	Positive: smaller liver lesions (in immunized animals)	Piedrafita et al., 2001; Sadeghi-Hashjin and Naem, 2001; Sibille et al., 2004
Echinococcus sp.	NO supports metacestode growth (*in vivo*)	N/A	NO killed protoscoleces (*in vitro*)	N/A	Amri et al., 2007; Amri and Touil-Boukoffa, 2015; Kanazawa et al., 1993; Mourglia-Ettlin et al., 2015; Zheng et al., 2016, 2017
Brugia malayi	N/A	NO, peroxynitrite immobilized microfilaria and L3 larvae (*in vitro*)	RNS reduced parasite burden (*in vivo*)	N/A	Gupta et al., 2004; Rajan et al., 1996; Taylor et al., 1996; Thomas et al., 1997;
Trichinella spiralis	N/A	N/A	RNS reduced parasite burden (*in vivo*)	Negative: more severe intestinal damage	Fabre et al., 2009; Hadas et al., 2001; Lawrence et al., 2000; Kołodziej-Sobocińska et al., 2006; Ming et al., 2016
Taenia crassiceps	N/A	N/A	RNS reduced parasite burden (*in vivo*)	N/A	Alonso-Trujillo et al., 2007
Strongyloides venezuelensis	N/A	NO immobilized L3 larvae and adults (*in vitro*)	RNS reduced parasite burden (*in vivo*)	N/A	Ruano et al., 2012
Toxocara canis	N/A	N/A	N/A	Positive: milder pulmonary damage	Espinoza et al., 2002

2.3. *Trichobilharzia regenti* and host immune response during vertebrate infections

T. regenti is a neuropathogenic avian schistosome that can also infect mice and other mammals which serve as accidental hosts. Cercariae penetrate the host's skin, transform into the stage of schistosomulum, find peripheral nerves and approximately 10% manage to migrate all the way to the central nervous system (CNS) (Hrádková and Horák, 2002; Kouřilová et al., 2004a). In ducks schistosomula get into the nasal cavity, where they mature and produce eggs (Hrádková and Horák, 2002). In mice, schistosomula occur in all spinal cord segments since 2 dpi until 24 dpi (Hrádková and Horák, 2002) and they never reach nasal cavity and/or mature (Horák et al., 1999).

In mice, neutrophils, macrophages, mast cells and CD4+ T-cells form inflammatory infiltrate around trapped schistosomula shortly after the skin penetration. These cells produce histamin and proinflammatory cytokines IL-1β, IL-6 and IL-12. Later, IFN-γ was found in both skin and skin-draining lymph nodes (Kouřilová et al., 2004a) possibly pointing to immune cells producing NO in the skin after cercarial penetration.

In immunocompetent mice, schistosomula tend to migrate to white matter of spinal cord even though the movement in it is probably more difficult (Bulantová et al., 2016; Kouřilová et al., 2004b). Even here they attract immune cells because inflammatory infiltrate was observed in spinal cord as well, mainly around damaged schistosomula. Macrophages/microglia dominate the periparasitic infiltrate in the CNS (Kouřilová et al., 2004a; Lichtenbergová et al., 2011). Hypertrophied astrocytes as well as glial scar can be found both in the infiltrate around damages parasites and in its migratory route (Lichtenbergová et al., 2011). In immunodeficient mice, however, schistosomula are found mostly in extraparenchymal sites where they can move without restrictions as the inflammatory infiltrate is not formed here (Kouřilová et al., 2004b). This suggests that by migrating to the white matter, schistosomula escape the immune system.

In vitro study on microglia and astrocytes showed that after stimulation with *T. regenti* derived stimulants (soluble fraction of LS homogenate, recombinant cathepsins B1.1 and B2), these cells produce NO and pro-inflammatory cytokines IL-6 and TNF-α. When schistosomula were cultivated with astrocyte culture, their motility and viability was markedly reduced. However, no elevation in nitrite concentration was measured in the culture medium (Macháček et al., 2016). Similarly, adding NOR-5, NO donor, to schistosomula *in vitro* did not significantly affect schistosomula viability and it also did not trigger significant changes in schistosomula ultrastructure. On the other hand, hydrogen peroxide significantly reduced parasite viability and caused severe changes in the

ultrastructure (Pankrác and Macháček, 2017) suggesting that mere NO does not affect schistosomula viability *in vitro* but for example peroxynitrite could.

Based on the review in the previous subchapter it is obvious that each helminthosis is unique and even though NO seems to be somewhat protective in schistosomosis, it doesn't necessarily mean that it is also protective in infection by the bird schistosome *Trichobilharzia regenti*, even though the causing agents are closely related. Although *in vitro* studies do not support the idea of NO relevance in these infections, *in vivo* results might be different as it is likely more complex immune interactions happen in the experimental mice and more experiments are necessary for establishing the role of NO or derived peroxynitrite in this infection.

3. Material and methods

The role of NO in *T. regenti* infections was explored by two approaches. We used *in vivo* experiments to determine if NO production is influenced by the infection and if NO affects the course of infection, whereas *in vitro* experiments were applied to evaluate the direct effect of peroxynitrite on schistosomula. Quantitative data were statistically analysed using GraphPad Prism 8.0 as stated directly in the chapter 4 (Results).

3.1. Buffers, media, solutions

Phosphate-buffered saline (PBS)

PBS (0.1 M, pH = 7.4) was a basic buffer used in most experiments as washing, dissolving or diluting agent. It was prepared fresh before each experiment from 10x concentrated stock solution (final composition of 1x PBS: 136.89 mM NaCl; 2.68 mM KCl; 4.23 Na_2HPO_4; 1.47 mM KH_2PO_4).

3.1.1. For *in vivo* experiments

Anaesthetics

Anaesthetic cocktail was prepared fresh under sterile conditions at room temperature in 1 ml insulin syringe for each experiment. The used components were:

- Sterile physiological saline (Mayrhofer Pharmazeutika)
- 10% (v/v) Rometar (Bioveta); final xylazine concentration: 2 mg/ml
- 20% (v/v Narketan (Vétoquinol); final ketamine concentration: 20 mg/ml

Anaesthetics were mixed well and 250-300 µl (depending on the size of the animal) were injected into the murine peritoneum.

Washing buffer for perfusions

Heparinized (10 U/ml, Heparin Zentiva) PBS was used as a washing buffer during perfusions (see 3.2.4.1.). It was warmed to 37 °C before use.

Fixative for perfusions

Fresh 4% (m/v) formaldehyde prepared by dissolving paraformaldehyde (Sigma Aldrich) in PBS at 70°C water bath was used as a fixative during perfusions (see 3.2.4.1.). Formaldehyde was cooled and kept on ice before use.

Permeabilizing buffer

Triton X-100 (Sigma Aldrich) was mixed with PBS to final 0.1% (v/v) concentration and used as a permeabilizing buffer during immunohistochemistry (IHC) (see 3.2.4.3.) and as a basic solution for blocking/incubation buffer.

Blocking/incubation buffer

Bovine serum albumin (BSA) was dissolved in permeabilizing buffer to make 1% (m/v) BSA, 0.1% (v/v) Triton X-100 solution. This solution was used for blocking slices and incubating them with antibodies during IHC (see 3.2.4.3.).

Antigen-retrieval buffer

Sucrose (Pentax) was dissolved in PBS to make 1% (m/v) sucrose solution and it was used for antigen retrieving on slices during IHC (see 3.2.4.3.) (Elias et al., 1990, cited from Shi et al., 1997; J. Bulantová, personal communication, 2017).

3.1.2. For *in vitro* experiments

Schistosomula cultivation medium (SCM)

SCM was prepared according to Vrbová (2017). It was used as a control cultivation medium during preliminary experiments and for the first part of schistosomula cultivation prior to treatment with SIN-1 (see 3.3.1.). SCM was prepared from ingredients listed in Table 2.

Table 2: Composition of 100 ml of SCM (adapted from Vrbová, 2017).

Chemicals	**Amount**	**Final concentration**
Basal Medium Eagle (BME) (Life Technologies)	100 ml	
Glucose (Sigma Aldrich)	0.1 g	111×10^{-4} M
HEPES (Sigma Aldrich)	0.24 g	1×10^{-3} M
Lactalbumin hydrolysate (Fluka)	0.1 g	0.1 % (w/v)
Hypoxanthine (Sigma Aldrich)	50 µl	5×10^{-7} M
Serotonin (Sigma Aldrich)	100 µl	1×10^{-6} M
Triiodothyronine (Sigma Aldrich)	100 µl	2×10^{-7} M
Hydrocortisone (Sigma Aldrich)	200 µl	1×10^{-6} M
Insulin (Sigma Aldrich)	800 µl	1.4×10^{-3} M
Schneider's Insect medium (Sigma Aldrich)	5 ml	5% (v/v)
MEM vitamins 100× (Life Technologies)	0.5 ml	0.5% (v/v)
BSA (Sigma Aldrich)	1 g	15×10^{-3} M
Antibiotic antimycotic solution 100× diluted (Sigma Aldrich)	1 ml	1% (v/v)

First, stock solutions of hormones and Schneider's Insect medium were prepared. Hormone stock solutions were prepared according to Table 3 and stored at -20 °C. Schneider's medium was dissolved in water (24.6 mg/ml) and 0.59 M $NaHCO_3$ was added to get the final concentration of 0.012 M. pH was measured using pH meter (inoLab, WTW) and adjusted to 9.2 by 1 M NaOH, then to 6.7 by 1 M HCl. In the end, 0.27 M $CaCl_2$ was added to get the final concentration of 0.0054 M and the solution was stored in darkness in 4 °C.

Table 3: Stock solutions of hormones (adapted from Vrbová, 2017).

Hormone	**Solvent**	**Stock solution concentration**
Hydrocortisone	96% (v/v) ethanol, then dH_2O added to make final concentration	1×10^{-3} M
Hypoxanthine	1M NaOH	1×10^{-3} M
Insulin	10^{-3} M HCl	0.17 M
Triiodothyronine	1M NaOH	2×10^{-4} M
Serotonin	10^{-4} M HCl	1×10^{-3} M

For SCM preparation according to Table 2, HEPES, glucose and lactalbumin hydrolysate were dissolved in 100 ml of BME. Hormones were added and pH was adjusted to 7.3–7.4 by 1 M HCl. Subsequently, Schneider's Insect medium, MEM vitamins and antibiotic antimycotic solution were added. In the end, pH was readjusted to 7.3–7.4 by 1 M HCl, osmolarity was measured using osmometer (Os3000, Marcel) and adjusted to 275 mOsm/kg by dH_2O. SCM was sterile filtered and stored at 4 °C before use.

Schistosomula cultivation medium based on M199

Given that hydrogen peroxide forms after peroxynitrite reacts with HEPES (Lomonosova et al., 1998), which is contained in SCM, it was necessary to use cultivation medium without this component. Thus, HEPES-free medium M199 (Howe et al., 2015) was enriched with antibiotic mixture, glucose and BSA according to Table 4 and was used for *T. regenti* schistosomula cultivation.

Table 4: Ingredients for 100 ml of cultivation medium M199 without phenol red and HEPES (Howe et al, 2015, modified).

Chemicals	**Amount**	**Final concentration**
M199 (ThermoFisher Scientific)	100 ml	
Antibiotic antimycotic solution 100× diluted (Sigma Aldrich)	1 ml	1% (v/v)
Glucose (Sigma Aldrich)	0.1 g	111×10^{-4} M
BSA (Sigma Aldrich)	1 g	15×10^{-3} M

Osmolarity and pH in the solution were measured using osmometer (Os3000, Marcel) and pH meter (inoLab, WTW) and adjusted to values 275 mOsm/kg by dH_2O and 7.3–7.4 by 1 M HCl, respectively, if necessary.

Washing buffer for electron microscopy (EM)

Washing buffer was used during sample preparation for both transmission (TEM) and scanning (SEM) EM (see 3.3.2.2.). First, twice concentrated 100 mM HEPES and 0.23 M NaCl stock buffer was prepared. Osmolarity and pH were measured using osmometer (Os3000, Marcel) and pH meter (inoLab, WTW) and adjusted to values 560 mOsm by dH_2O and 7.0 by 1 M HCl, respectively. Stock solution was diluted twice before use.

Fixative for EM

Fixative for EM (see 3.3.2.2.) was prepared by mixing 5 % glutaraldehyde in H_2O with stock washing buffer for EM in 1:1 ratio.

Spurr embedding medium for TEM

Embedding medium for TEM (see 3.3.2.2.) was prepared using Spurr Low-Viscosity Embedding Kit (Polysciences, Inc.) according to Table 5. First, ERL 4221, diglycidyl ether of polypropylene glycol (D.E.R. 736) and nonenyl succinic anhydride (NSA) were carefully weighted and gently mixed. Then dimethylaminoethanol (DMAE) was added and the medium was gently mixed again. The medium was stored at -20 °C before use.

Table 5: Ingredients for Spurr embedding medium

Chemicals	Amount
ERL 4221	4.10 g
D.E.R. 736	1.43 g
NSA	5.90 g
DMAE	0.10 g

3.2. *In vivo* experiments

In *in vivo* experiment mice infected with *T. regenti* were used. The amount of NO produced during infection was evaluated on a systemic level by measuring nitrites/nitrates in blood sera using Griess reaction (see 3.2.2.). NO production and nitrosative stress levels in the affected tissues, namely skin and spinal cord, were assessed by detecting iNOS and 3-NT using immunohistochemistry (IHC) (see 3.2.4.3.). To test if NO affects parasite burden in the spinal cord and demyelination, mice were treated by iNOS inhibitor prior and during the infection (see 3.2.3.2.). Timepoints were chosen according to previous experiments performed in our laboratory. Experimental design of *in vivo* experiments is summarized in Figure 5.

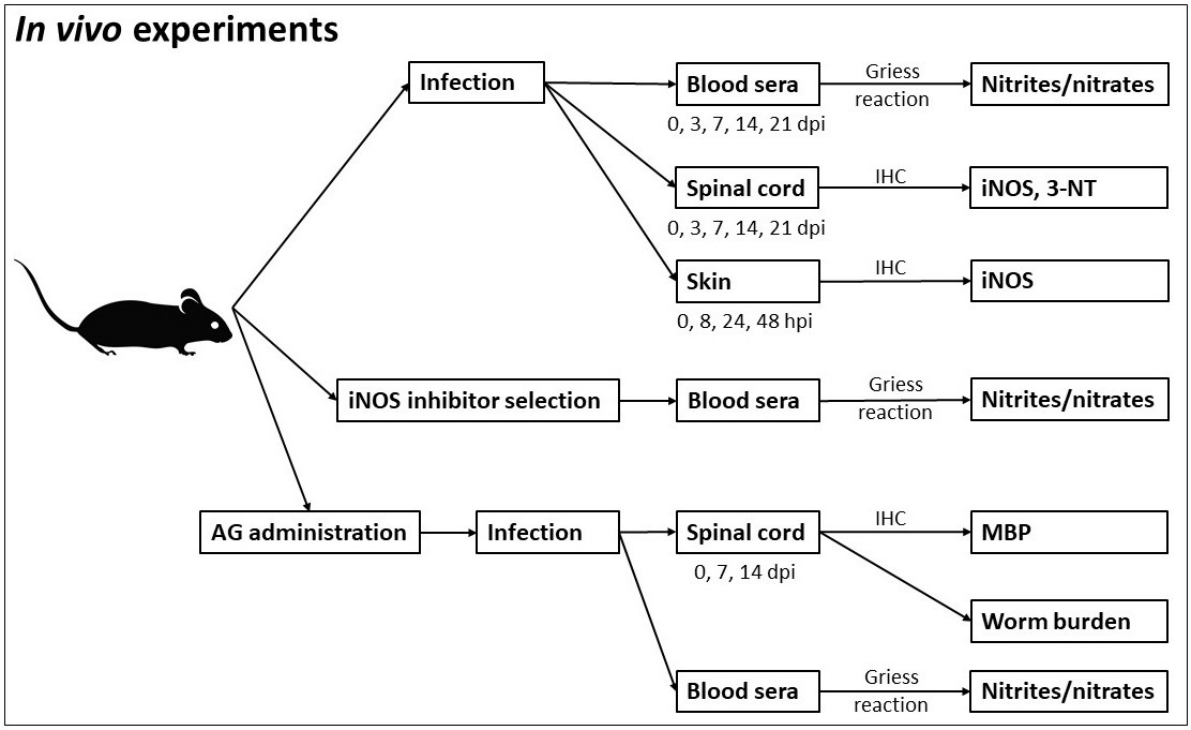

Figure 5: Summary of designs of in vivo *experiments.* Abbreviations: dpi – days post infection; hpi – hours post infection; IHC – immunohistochemistry; iNOS – inducible NO synthase; 3-NT – 3-nitrotyrosine; AG – aminoguanidine (NOS inhibitor); MBP – myelin basic protein

3.2.1. Animals and manipulation

3.2.1.1. *Trichobilharzia regenti*

T. regenti life cycle is maintained at the Department of Parasitology, Faculty of Science, Charles University, using *Radix lagotis* as an intermediate host and *Anas platyrhynchos* f. *domestica* as a final host. To obtain cercariae for experimental infections, snails were collected into container with still water illuminated by lamps, which stimulated shedding cercariae. After 60 minutes these were collected and put into almost fully covered beaker to concentrate them using their positive phototaxis. Concentrated cercariae were then counted in 20 x 50 µl to calculate their number per

ml. Infection doses were prepared by mixing volume containing 2000 cercariae with still water to the final volume of 50 ml for systemic infection. In case of pinnae infection, the infection dose was 500 cercariae in 1.5 ml of still water.

3.2.1.2. Infection of accidental hosts

Female mice of the strain C57BL/6JOlaHsd (ENVIGO), 8 weeks old, were used as experimental accidental hosts. Mice were kept in conventional boxes under standard conditions (23 °C, 55% humidity, 12/12 light/dark mode, food and water provided *ad libitum*) in the Centre for Experimental Biomodels, 1st Faculty of Medicine, Charles University.

Preceding systemic infections, each mouse was put into 500 ml dark beaker containing approximately 40 ml of water for 30 minutes to defecate and urinate. Infections took place in the same washed beakers, only the water was exchanged for 50 ml of still water containing the infection dose. After 60 minutes, when cercariae were penetrating the skin of submerged tails and legs, infections were complete, and mice were put back into the boxes.

In case of the pinnae infection, mice were anaesthetized using ketamine/xylazine as described below, laid on a microtube stand with left pinnae submerged in dark Eppendorf tube with infection dose of cercariae. Mice were moved to their boxes 15 minutes later and checked until they recovered from anaesthesia. Mice were sacrificed at given timepoints (see Figure 5) and non-infected mice (0 dpi) were always used as a biological negative control.

3.2.1.3. Anaesthesia

Two types of anaesthetics were used during *in vivo* experiments. An inhalation anaesthesia by isoflurin (1000 mg/g isofluranum in stock solution; Vetpharma animal health) was used during experiment including iNOS inhibitors (see 3.2.3.1. and 3.2.3.2.). In other experiments mice were i.p. anesthetized by 250-300 µl of anaesthetics cocktail, depending on their size and weight.

3.2.1.4. Ethics statement

All experiments were performed in accordance with animal welfare laws of Czech Republic and the directives of the European Union and were approved by the Animal welfare committee of Faculty of Science, Charles University, and by the Ministry of Education, Youth and Sports (MSMT-31114/2013-9). Handling animals was always performed or supervised by a person authorized to design and perform the experiments with animals according to section 15d (3) of Act No. 246/1992 Coll.

3.2.2. Griess reaction for measuring nitrite/nitrate levels

Nitrite/nitrate levels were measured in sera samples using Griess reaction during both non-treated and AG treated *T. regenti* infections. The method was also applied during testing iNOS inhibitors (see 3.2.3.1.).

Blood samples were collected shortly before transcardial perfusion (see 3.2.4.1.) after cutting right atrium. To obtain sera, clotted blood samples were centrifuged for 10 minutes at 1500 g. Amicon Ultra-0.5 Centrifugal Filter Unit, 10 kDa (Merck) were hydrated with 100 µl of ultra-pure water by centrifugation for 10 minutes at 14000 g. Serum samples, 100 µl each, were loaded onto the hydrated filter units and deproteinated by ultra-centrifugation for 30 minutes at 14000 g. Nitrite/nitrate levels in deproteinated sera were measured in a 96-well plate using Nitrite/Nitrate Colorimetric Assay Kit (Cayman Chemical) following the manufacturer's assay protocol. Briefly, samples and standards (0, 5, 10, 15, 20, 25, 30, 35 µM nitrate) were loaded into the wells, nitrates were reduced to nitrites during incubation with nitrate reductase for 3 hours at room temperature, Griess reagents were added and absorbance was read at 550 nm using a plate reader Tecan infinite M200.

3.2.3. iNOS inhibitor treatment

To examine the effect of NO on the course of *T. regenti* infection, an iNOS inhibitor was chosen for mice treatment. Afterwards, worm burden and the level of demyelination was examined (see 3.2.4.2. and 3.2.4.4.).

3.2.3.1. Testing different iNOS inhibitors

In this preliminary experiment, the effect of several iNOS inhibitors on NO production was tested. AG, L-NIL and N-[[3-(aminomethyl)phenyl]methyl]-ethanimidamide (1400W) were administered to healthy mice prior to or concurrently with LPS (5 mg/kg; in sterile PBS) (see Table 6). First control group received received PBS instead of LPS or inhibitors, second control group only received LPS injections without inhibitors. Sera samples for measuring nitrites/nitrates levels were obtained 6 hours after the LPS injection. Mice were anesthetized using isoflurin, blood samples were collected after cutting aorta and processed as described in subchapter 3.2.2.

Table 6: Summary of used NOS inhibitors, dosage and application schedule.

Inhibitor	Abbreviation	Dosage	Application	Reference
Aminoguanidine hydrochloride (Sigma Aldrich)	AG	50 mg/kg	24 hours before LPS, with LPS	Kolodziej-Sobocinska et al., 2006
N6-(1-iminoethyl)-L-lysine (Sigma Aldrich)	L-NIL	5 mg/kg	1 hour before LPS	Schweighöfer et al., 2014
N-[[3-(aminomethyl)phenyl]methyl]-ethanimidamide (Sigma Aldrich)	1400W	20 mg/kg	1 hour before LPS	Lee et al., 2015

3.2.3.2. AG treatment

Based on preliminary experiments, AG was chosen for iNOS inhibition during *T. regenti* infection. Mice were divided into groups according to Table 7 and groups 2A-3B were infected as described above (see 3.2.1.2.) one day after AG/control treatment had started. Non-infected mice of groups 1A and 1B were used as a biological control and otherwise treated as groups 2A and 2B. "B" groups received 100 µl of freshly prepared AG dissolved in sterile PBS (10 mg/ml) i.p. each morning for 8 or 15 days (see Table 5) starting one day before infection. "A" groups received the same doses of PBS only to assess the effect of AG treatment and were sacrificed together with corresponding "B" groups. Mice were then processed as described below, including measuring sera nitrite/nitrate levels described in 3.2.2.

Table 7: Characteristics of groups of mice used for AG-treated infections. Abbreviations: "+" – yes (the group was infected or AG treated); "–" – no (the group was non-infected or PBS treated).

Group no.	Infection	Duration of infection (dpi)	Treatment	No. of days of treatment	Name of group
1A	–	–	PBS	8	0 PBS
1B	–	–	AG	8	0 AG
2A	+	7	PBS	8	7 PBS
2B	+	7	AG	8	7 AG
3A	+	14	PBS	15	14 PBS
3B	+	14	AG	15	14 AG

3.2.4. Immunohistochemistry

IHC staining was applied on the murine spinal cord frozen tissue sections to:

a) Analyse the presence of iNOS and 3-NT. This was done in the samples from 0, 3, 7, 14 and 21 dpi as the dynamics of iNOS and 3-NT during infection was of interest.
b) Mark astrocytes and microglia and decide if they produce iNOS based on colocalization with iNOS signal. This was done only in the samples from 3 dpi where the strongest iNOS signal was observed. Glial fibrillary acidic protein (GFAP) and ionized calcium-binding adaptor molecule (Iba-1) were chosen as astrocytic or microglial markers, respectively.
c) Detect changes in demyelination after *T. regenti* infection and inhibition of iNOS with AG. This was done in the samples from 0, 7 and 14 dpi where we observed both intact and damaged schistosomula. The level of tissue myelination was detected by MBP staining as demyelination would lead to smaller amount of detected MBP.

Moreover, IHC was applied to analyse the presence of iNOS in the pinnae skin. 3-NT was not detected in the skin due to lack of pAb.

3.2.4.1. Transcardial perfusion

A deeply anesthetised mouse was fixed to the dissection board and thorax was carefully cut open. 25G needle, a part of a perfusion apparatus, was carefully inserted into the left ventricle and right atrium was cut open. At this point blood samples for measuring nitrites/nitrates were collected (for their processing see 3.2.2.). After collecting blood, approximately 40–50 ml of washing buffer were slowly pushed into the murine circulatory system. Decolorization of the liver was the sign of a successful washing part of perfusion. Similar volume of the fixative was then pushed into the circulation and "formalin dance" proved successful fixative penetration.

3.2.4.2. Tissue samples preparation

The spine was dissected after perfusion, cleared of as much muscle tissue as possible and post-fixed in fixative (4% formaldehyde prepared before perfusions) for approximately 15 minutes. Spinal cord was carefully cut out of the spine and separated into 4 segments: cervical (ending between C7 and Th1 vertebrae), thoracic (ending between Th10 and Th11 vertebrae), lumbar (ending between L1 and L2 vertebrae) and sacral (caudally from L2 vertebra). Each segment was post-fixed overnight in 2 ml of 4% formaldehyde in 4 °C.

Mice with infected pinnae were sacrificed by cervical dislocation, pinnae were cut off and post-fixed overnight in 5 ml of 4% formaldehyde in 4 °C each.

After this, the spinal cord segments and pinnae were washed with PBS for 3x15 minutes and cryoprotected using rising concentrations of sucrose (Pentax) in PBS. Tissue was first incubated in 10% (m/v, in PBS) sucrose solution for up to 2 hours, then in 20% (m/v, in PBS) sucrose solution for up to 6 hours and finally in 30% (m/v, in PBS) sucrose solution overnight. Tissue sinking was a clear marker of proper saturation with sucrose and each step was finished after all samples were on the bottom of the tubes. The samples were then embedded in Tissue Freezing Medium (Leica Biosystems) and stored in freezing molds (Leica Biosystems) in -20 °C overnight. If longer storage (4 months maximum) was necessary, samples were moved to -80 °C.

Using cryostat (Leica Biosystems CM3050S) set to -20 °C, 10 µM slices were prepared from the frozen tissue samples. Slices were transferred onto adhesive Xtra slides (Leica Biosystems) and checked for schistosomula presence under a light microscope and schistosomula were counted in spinal cords dedicated to MBP staining. Schistosomula-positive slides, later used for IHC, were then stored in -80 °C (4 months maximum).

3.2.4.3. IHC staining

Schistosomula-positive slides were tempered in room temperature, tissue was framed using hydrophobic NovoPen (Leica Biosystems) and washed 3x10 minutes with PBS in wet chambers. When MBP was detected, slides were incubated with permeabilization buffer for 10 minutes. Blocking buffer was implemented in all staining protocols to block non-specific binding and slides were incubated with this buffer for 60 minutes. When other targets than MBP (see Table 8) were detected, antigen-retrieving buffer was applied for 22 hours at 4 °C. The following steps were identical for all targeted antigens. Slides were washed 3x10 minutes with PBS and incubated with primary antibodies (see Table 8) in incubation buffer overnight in 4 °C. After that, the slides were washed 6x5 minutes with PBS and following steps were performed in the dark. Secondary antibodies (see Table 8) in incubation buffer were added for one hour and then the slides were washed 6x5 minutes with PBS. Finally, the slides were mounted in 30 µl of VectaShield containing 4',6-Diamidine-2'-phenylindole (DAPI). The slides were examined and photographed using a fluorescent microscope (Olympus BX51) equipped with the camera (Olympus DP-2). Photographs were then processed using Quick Photo Micro 3.0 and Gimp 2.8. Slides stained for microglia/astrocytes markers and iNOS were observed and photographed using inverted confocal microscope Zeiss LSM 880. ZEN Black and ImageJ were used for processing photographs.

Table 8: Overview of antibodies used in IHC. Abbreviations: TFS = ThermoFisher Scientific; CST = Cell Signalling Technology; AF = Alexa Fluor.

Target	Vendor	Clone	Host	Dilution	Secondary antibody	Dilution
iNOS	TFS	polyclonal	rabbit	1:500	goat anti-rabbit AF 594 (TFS)	1:1000
MBP	TFS	polyclonal	rabbit	1:1000		
3-NT	Abcam	39B6	mouse	1:200	donkey anti-mouse AF 488 (TFS)	1:1000
GFAP	CST	GA5	mouse	1:600		
Iba-1	Synaptic systems	polyclonal	rabbit	1:1000	goat anti-rabbit AF 488 (TFS)	1:1000

Rabbit primary antibodies specificity was tested by their substitution with negative rabbit serum (Dako) in the same concentration as the rabbit antibodies (1:500). When the specificity of secondary antibodies was tested, only incubation buffer was used instead of secondary antibodies. The rest of the staining steps were performed as described above.

3.2.4.4. Signal quantification

To examine tissue demyelination, the MBP signal was quantified. To ensure optimal conditions for image processing, all MBP-stained slides were captured at 200x magnification for 1/300 s. Pictures were sent to the Laboratory of Confocal and Fluorescence Microscopy, Faculty of Science, Charles University, Prague for image analysis (performed by Ing. Martin Schätz). Briefly, the pictures were

transformed into black-and-white format and their histograms were normalized using R Studio. Median fluorescence intensities within the groups (see Table 7) were compared between tested groups.

3.3. *In vitro* experiments

The main goal of *in vitro* experiments was to evaluate the effect of peroxynitrite on *T. regenti* schistosomula. First, new cultivation medium was tested. Then, schistosomula were cultivated with SIN-1, the donor of peroxynitrite (see 3.3.2.). Schistosomula viability was then established by two approaches, methylene blue staining and lactate levels measurements (see 3.3.2.1.). Schistosomula were also processed for electron microscopy imaging (see 3.3.2.2.) to examine their damage caused by peroxynitrite.

3.3.1. Preparation of *T. regenti* schistosomula

T. regenti cercariae were collected as described above (see 3.2.1.1.) and immobilized on ice for 1 hour. This process concentrated them on the bottom of the tubes. Redundant water was removed until approximately 5 ml containing cercariae was left. These were mechanically transformed into schistosomula as described by Chanová et al. (2009). Briefly, cercariae were passed through a syringe (10 ml volume, 0.6 mm diameter) at least 20 times. Cercarial bodies were then put into a Petri dish and washed three times with SCM to remove detached cercarial tails. During washing, the cercarial bodies were concentrated in the middle of the Petri dish by gyratory movement of the dish and the medium with detached tails was drawn out on the side of the Petri dish. The cercarial bodies were incubated in SCM overnight (37 °C, 5% CO_2). After the overnight incubation in SCM, the transformed schistosomula were cultivated either in M199 or SCM in 37 °C, 5% CO_2. The motility of schistosomula was observed under microscope after 2, 4, 6, 8, 10, 24 and 48 hours. M199 was used in subsequent experiments.

3.3.2. Schistosomula cultivation with SIN-1

After the transformation and overnight incubation in SCM, schistosomula (30 individuals per well, final volume: 500 µl of M199) were cultivated in 24-well cultivation plates (BioFil) and 3 experimental groups were created (see Table 8). SIN-1 was dissolved in M199 (3 mM stock solution) and added to wells of groups 1, 2, 4 and 5 as described in Table 9. Group 3 served as a biological negative control, whereas groups 4 and 5 served as a SIN-1 background control. Media samples for lactate measurement were collected after 48 hours, deproteinated by centrifugation using hydrated filter units as described in 3.2.2. and stored at -80 °C. Schistosomula viability was established using methylene blue staining.

Table 9: Summary of groups included in evaluating the effect of peroxynitrite on schistosomula.

Group no.	Schistosomula	SIN-1
1	30 individuals	3 mM
2	30 individuals	1.5 mM
3	30 individuals	0 mM
4	0	3 mM
5	0	1.5 mM

3.3.2.1. Assessment of schistosomula viability

Lactate measurement

Levels of lactate in deproteinated media samples were measured in 96-well plates using L-Lactate Assay Kit (Colorimetric/Fluorometric) (Abcam) according to the manufacturer's protocol for fluorometric detection. Briefly, 50 µl of diluted media samples (1:49 in assay buffer) and L-Lactate standards (0, 20, 40, 60, 80 and 100 pmol) were mixed with the equal volume of enzyme mix and fluorescent probe. The plate was then incubated at room temperature for 30 minutes protected from light. Output was measured by the microplate reader Tecan infinite M200 (ex/em = 535/587 nm).

Methylene blue staining

Methylene blue (0.03%, m/v, in Earle's saline) was added to schistosomula in medium so that the final ratio of dye and medium was 1:1. After 10 minutes, schistosomula were washed by PBS to get rid of methylene blue and examined under the stereomicroscope on both dark and light background (Nikon SMZ645). Viable schistosomula remained unstained, while dead schistosomula were blue (Li Hsü et al., 1977). Schistosomula had to be medium dark blue to be considered dead. Schistosomula were counted and percentage of viable (unstained) schistosomula was calculated.

3.3.2.2. Schistosomula processing for electron microscopy

First part of the protocol was identical for SEM and TEM. Methylene blue stained schistosomula were washed 3x10 minutes using washing buffer and fixed at 4 °C overnight. Fixative was washed out 3x10 minutes with washing buffer and samples were post-fixed in 4% (v/v) OsO_4 in washing buffer for 1 hour. Afterwards, samples were properly washed 3x10 minutes with washing buffer and dehydrated using ethanol and acetone. Samples were incubated for 10 minutes in 30, 50, 70 and 80% ethanol and for 5 minutes in 90, 96 and 3x 100% ethanol and 3x 100% acetone.

SEM

Immediately after dehydration samples were sent to Electron Microscopy Lab, Faculty of Science, Charles University (EML) to be dried by liquid CO_2 in CPD 030 (performed by RNDr. Miroslav Hyliš,

Ph.D.). Schistosomula were then arranged on a tag on a cylinder used for SEM imaging. Schistosomula were observed and photographed using JEOL 6380 LV microscope. Photographs were then processed using GIMP 2.8.

TEM

After dehydration, samples were incubated in solution of Spurr and acetone, 3:1 ratio, for 2 hours. The solution was exchanged for solution of Spurr and acetone, 1:1 ratio, for 4 hours and then solution of Spurr and acetone, 1:3 ratio, was used for overnight incubation. Samples were incubated with Spurr for 12 hours and embedded in fresh Spurr for polymerization at 60 °C for 48 hours. Samples were then sent to EML to be cut to ultrathin slices. Samples were observed and photographed using JEOL 1011 microscope. Photographs were then processed using GIMP 2.8.

4. Results

4.1. *In vivo* experiments

4.1.1. Nitrites/nitrates in sera

Nitrites/nitrates were measured in sera from *T. regenti* infected mice (at 0, 3, 7, 14 and 21 dpi) using Griess reaction to examine NO production on a systemic level. For each timepoint, sera samples from 7 mice were used, 3 of which were also processed for IHC staining (see 3.2.4.). Remaining 4 samples were obtained from mice infected as described above but used for a different study. No striking trend was noticed in nitrites/nitrates serum levels throughout the infection (Figure 6) and they did not differ significantly (one-way ANOVA: F (4,29) = 1.976; P = 0.1247).

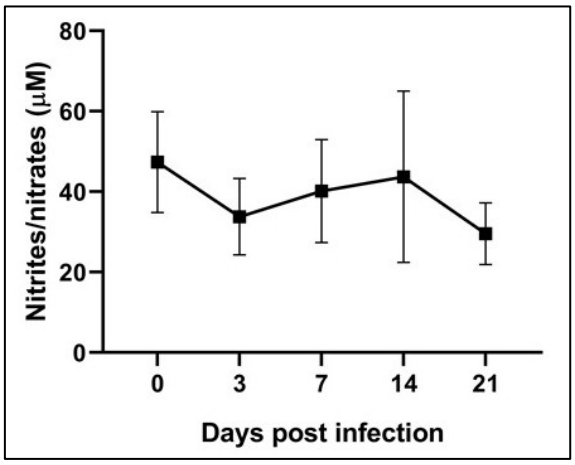

Figure 6: Nitrite/nitrate levels (μM) in sera samples obtained from T. regenti *infected mice at 0, 3, 7, 14, 21 days post infection (dpi), n = 7 for each timepoint.* No statistically significant differences were found (one-way ANOVA; F (4,29) = 1.976; P = 0.1247). Data are shown as mean ± standard deviation.

4.1.2. iNOS and 3-NT detection by IHC

NO production in the infected pinnae was examined by IHC iNOS staining at 0, 8, 24 and 48 hpi. For each timepoint, 3 mice were infected and processed for IHC. No schistosomula were found at 24 hpi, therefore the presence of iNOS could not be examined at this timepoint. For timepoints 8 and 48 hpi, 5 schistosomula-positive slides were stained; 5 slides were also used as a control (0 hpi). iNOS signal was observed in the upper skin layers of pinnae close to the parasite at 8 hpi but not at 48 hpi (for summary see Table 10). Representative pictures of infected and control pinnae with stained iNOS and nuclei are shown in Figure 7.

Figure 7 (see page 35): Representative pictures of stained iNOS in infected pinnae at 0 (A, B), 8 (C, D) and 48 (E, F) hpi. Three mice per timepoint were infected and at least 6 schistosomula-positive slides per timepoint were examined. Left column shows pictures with merged nuclei (stained by DAPI) signal (blue) and iNOS (red) for better orientation in the tissue, whereas right column only shows iNOS signal. Abbreviations: hpi – hours post infection; iNOS – inducible NO synthase; * - *T. regenti* schistosomulum (also stained by iNOS pAb).

Table 10: Summary of schistosomula-positive slides with positive signal for iNOS. Five slides per timepoint were examined. Abbreviations: hpi – hours post infection; iNOS – inducible NO synthase.

Timepoint	iNOS positive signal (positive slides/all slides)
0 hpi	0/5
8 hpi	4/5
24 hpi	N/A (no schistosomula detected)
48 hpi	0/5

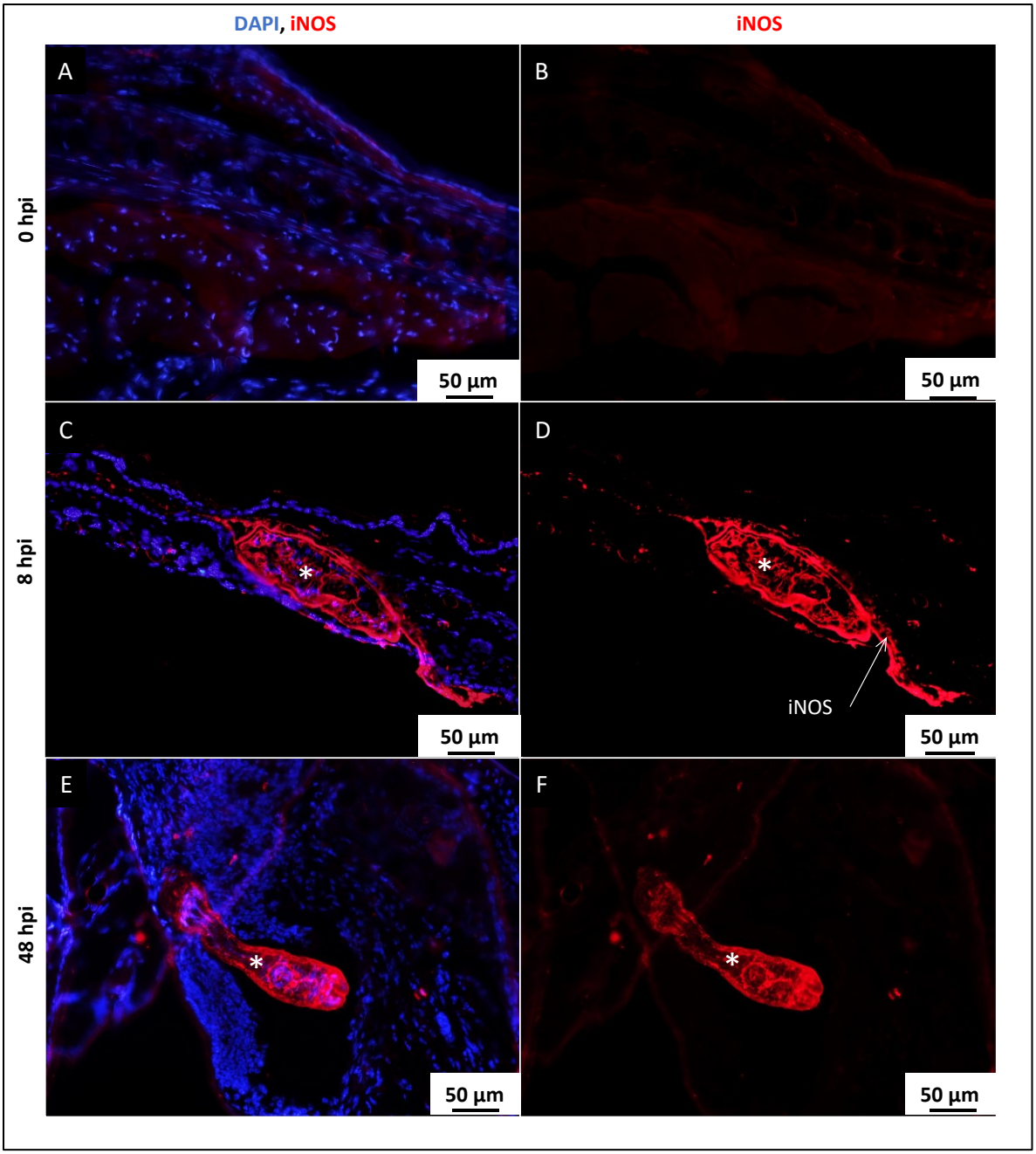

Figure 7: Representative pictures of stained iNOS in infected pinnae at 0 (A, B), 8 (C, D) and 48 (E, F) hpi. For further description see page 34.

Besides pinnae, iNOS was also detected in infected spinal cords at 0, 3, 7, 14 and 21 dpi (3 mice per each group were used). 3-NT was also detected in these samples. At least 2 schistosomula-positive slides per mouse were used for iNOS and 3-NT detection. iNOS with rather diffused pattern lacking a specific cellular localisation was often detected in a vicinity of the parasite at 3 dpi and once at 7 dpi. On the other hand, 3-NT was detected seemingly around nuclei in the tissue around the parasite at later timepoints (for representative pictures see Figure 8). In some cases, 3-NT was detected even within the parasite internal tissues showing the similar perinuclear localisation. Frequency of positive signal for iNOS and 3-NT (positive slides/all stained slides with schistosomula) is summarized in Table 11.

Table 11: Summary of schistosomula-positive slides with positive signal for iNOS or 3-NT. Three mice per group were infected, at least 2 schistosomula-positive slides per mouse were examined. Abbreviations: dpi – days post infection; iNOS – inducible NO synthase; 3-NT – 3-nitrotyrosine.

Timepoint	Positive signal (positive slides/all slides)		
	iNOS	3-NT in tissue	3-NT within parasite
0 dpi	–	–	–
3 dpi	13/21	–	–
7 dpi	1/14	11/14	2/14
14 dpi	–	13/16	5/16
21 dpi	–	7/9	4/9

Colocalization of 3-NT and DAPI signals was further examined using confocal microscopy to determine the affected cellular structures. This analysis showed 3-NT signal around nuclei rather than within them (Supplementary Figure S1A), nevertheless, the results were inconclusive and would require better sample processing and/or different imaging technique. Additionally, colocalization of iNOS with astrocytes and microglia was also examined in order to identify the cellular source of the iNOS. However, the iNOS signal did not overlap either with that of GFAP (astrocytes marker) or Iba-1 (microglia marker) (Supplementary Figure S1B and S1C).

Figure 8 (see page 37): Representative pictures of stained iNOS (red) and 3-NT (green) in the infected spinal cord (red) at 0 (A, B), 3 (C, D), 7 (E, F), 14 (G, H) and 21 (I, J) dpi with parasites stained by iNOS pAb (red). Three mice per timepoint were used and at least 2 schistosomula-positive slides per mouse were examined. The left column shows pictures with stained nuclei (blue) and iNOS (red) for better orientation in the tissue, whereas right column shows only pictures of red and green signal for clear view of the stained molecules. Abbreviations: iNOS - inducible NO synthase; 3-NT – 3-nitrotyrosine; dpi – days post infection; * - schistosomulum *T. regenti* (also stained by iNOS pAb).

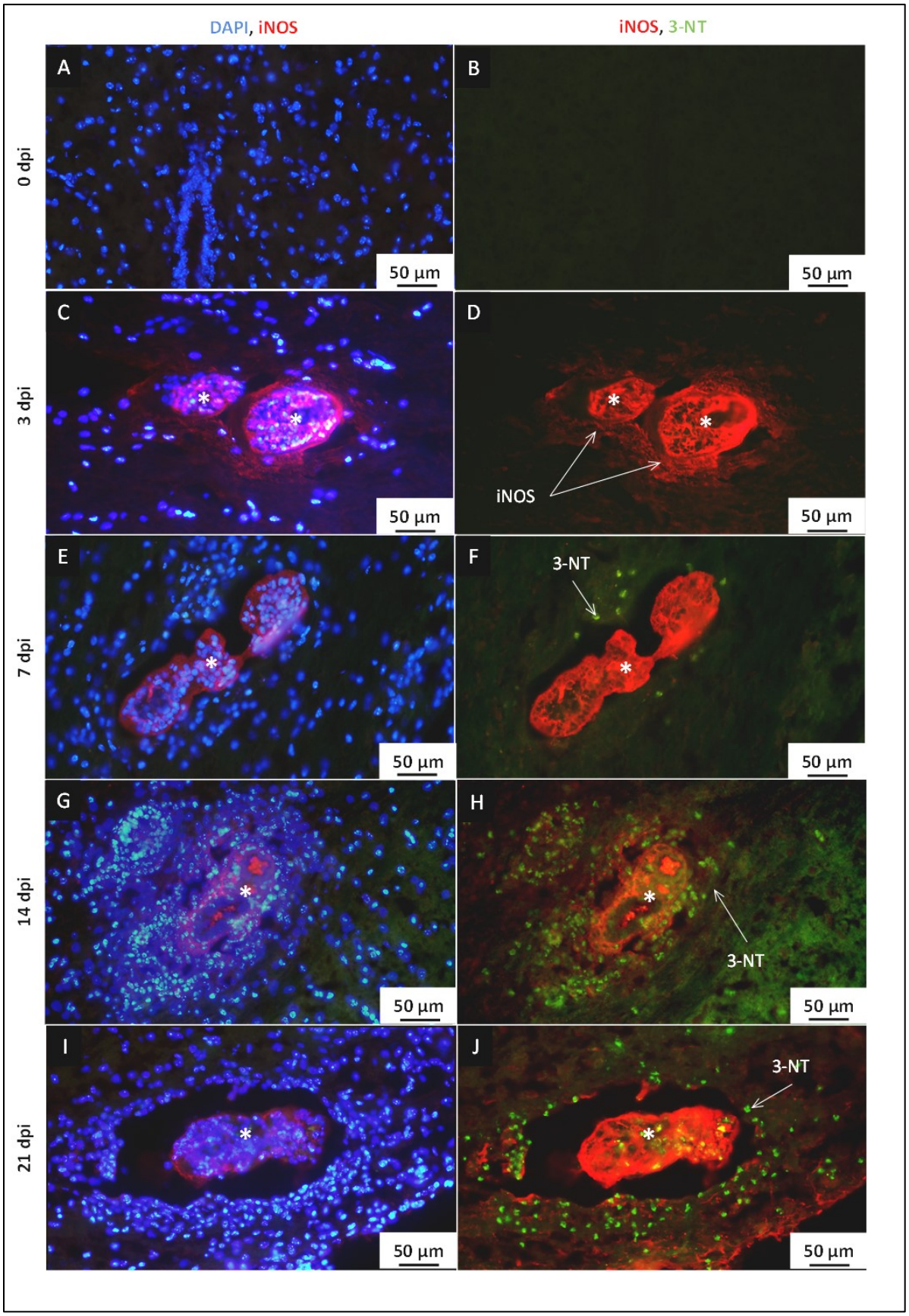

Figure 8: Representative pictures of stained iNOS (red) and 3-NT (green) in the infected spinal cord.
For further description see page 36.

4.1.3. AG treatment

4.1.3.1. Inhibitor testing

In this preliminary experiment, we tested the efficacy of three iNOS inhibitors to choose the best one to be applied in subsequent experiments. Although only 3 mice per group were used, we were able to evaluate the inhibitor efficacy by measuring nitrite/nitrate levels in sera after LPS treatment. As shown in Figure 9A, LPS treatment triggered NO production resulting in a significant increase in serum nitrite/nitrate levels, which was significantly diminished if the mice were concurrently treated with any of the inhibitors (L-NIL, 1400W, AG). However, neither of them lowered the serum nitrites/nitrates levels to those of untreated animals, even though there were no significant differences between untreated and L-NIL- or 1400W-treated animals. P values for all performed comparisons (Sidak's multiple comparisons test) are shown in Figure 9B. Based on the results, availability and price of the inhibitors, AG was chosen to be used in further experiments.

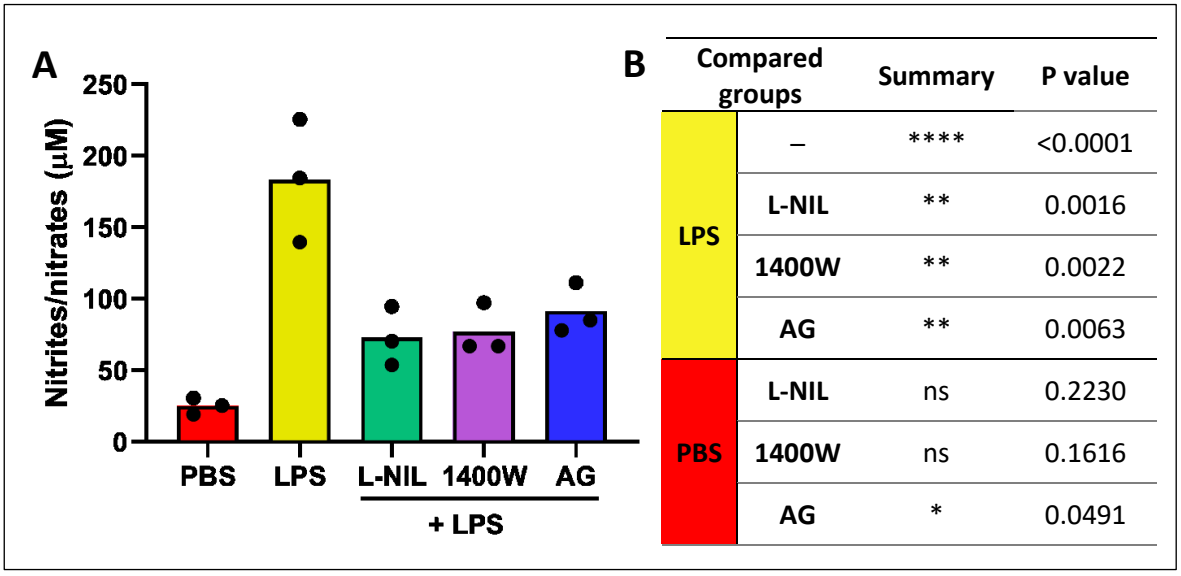

B

Compared groups		Summary	P value
LPS	–	****	<0.0001
	L-NIL	**	0.0016
	1400W	**	0.0022
	AG	**	0.0063
PBS	L-NIL	ns	0.2230
	1400W	ns	0.1616
	AG	*	0.0491

Figure 9: Nitrite/nitrate levels (µM) in sera obtained from mice (n = 3 mice per group) treated 6 hours with LPS (5 mg/kg) and iNOS inhibitors L-NIL (5 mg/kg), 1400W (20 mg/kg) and AG (50 mg/kg). A: Nitrite/nitrate levels as measured by Griess reaction. Data are shown as mean and individual values. *B: Summary of statistical analysis by one-way ANOVA (F (4, 10) = 17.19; P = 0.0002)) followed by Sidak's multiple comparisons test.* Abbreviations: PBS – negative control; LPS – positive control; L-NIL- N6-(1-iminoethyl)-L-lysine; 1400W - N-[[3-(aminomethyl)phenyl]methyl]-ethanimidamide**;** AG – aminoguanidine.

4.1.3.2. The effect of AG on the course of infection

The effect of AG on the course of infection was tested at 0 (n = 2 mice per group), 7 (n = 3 mice per group) and 14 (n = 3 mice per group) dpi. In particular, number and localisation of schistosomula in the spinal cord and demyelination of the tissue were in focus.

After transcardial perfusion and tissue processing, schistosomula were counted in the spinal cord segments (cervical, thoracic, lumbar and sacral segments) during slide examination immediately after cryosectioning. As shown in Figure 10, there was a trend towards more parasites at the earlier timepoint (7 dpi) and in PBS-treated groups (two-way ANOVA; time: F (1,8) = 37.36; P = 0.0003; treatment: F (1,8) = 8.022; P = 0.0221), but the values from particular comparisons (control vs. AG group) were on the verge of significance (Holm-Sidak's test; 7 dpi: p = 0.0956; 14 dpi: p = 0.1302). AG treatment also did not cause significant changes in the parasite distribution in the spinal cord segments (see Table 12) (Fisher's test; 7 dpi: P = 0.3346; 14 dpi: P = 0.3141). Summary of parasite burden reflecting schistosomula distribution within the spinal cord is stated in Supplementary Table S1.

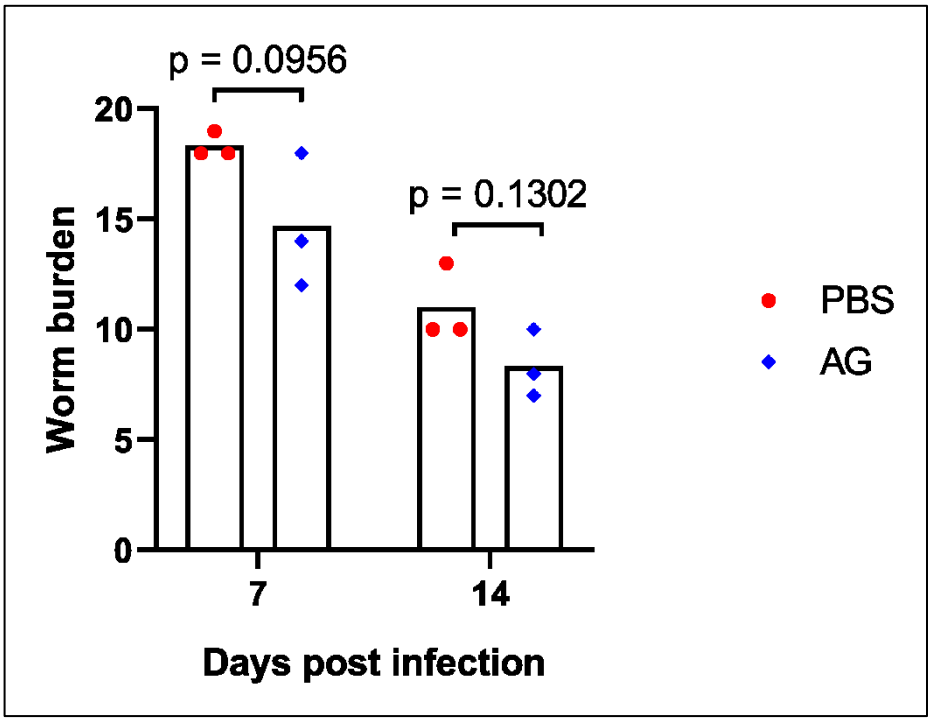

Figure 10: Average schistosomula burden per group (n = 3 mice per group). Data are shown as mean and individual values. Two-way ANOVA showed significant effect of both time (P = 0.0003) and treatment (P = 0.0221). However, Holm-Sidak's multiple comparisons test didn't show any significant difference between PBS- and AG-treated groups.

Table 12: Summary of schistosomula burden in spinal cord segments (n = 3 mice per group) found on the slides immediately after cryosectioning. The sums of numbers obtained from all mice from groups, n = 3 mice per each group, are stated in the table. Fisher's test (7 dpi: P = 0.3346; 14 dpi: P = 0.3141) did not reveal any significant differences between schistosomula burden in PBS- and AG-treated groups.

Spinal cord segment	7 dpi		14 dpi	
	PBS	AG	PBS	AG
Cervical	12	8	11	4
Thoracic	32	23	13	11
Lumbar	9	13	9	10
Sacral	2	0	0	0
Sum	55	44	33	25

Besides assessing schistosomula burden, their localization within the spinal cord (grey matter, white matter, submeningeal spaces) was examined in the subset of schistosomula-positive slides undergoing MBP staining (see 4.1.3.3.). The parasite distribution within the spinal cord (regardless the length of the infection, i.e. Figure 11 shows pooled schistosomula number) was not significantly affected by AG treatment (Fisher's test; P = 0.1418).

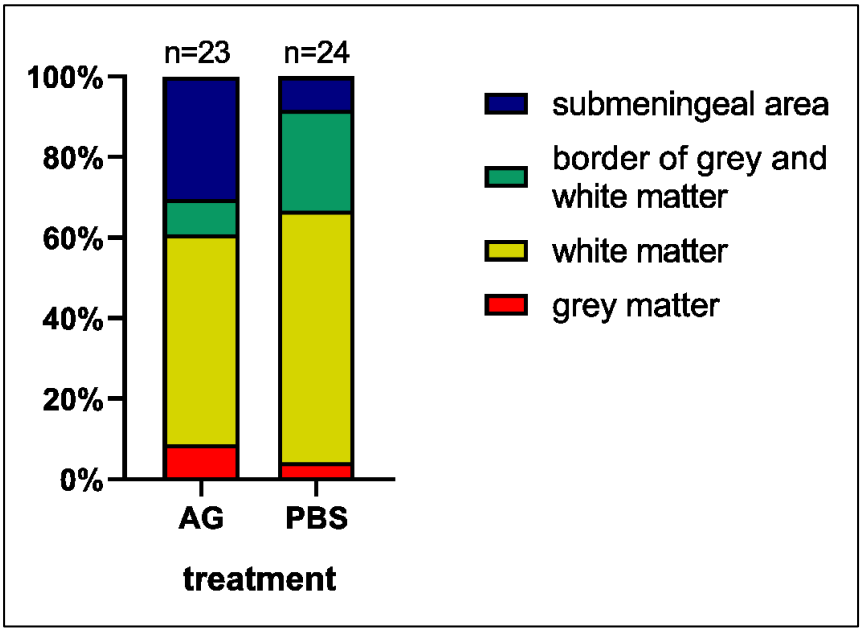

Figure 11: Relative representation of schistosomula burden per localization within the spinal cord segment examined on MBP-stained slides. Fisher's test (P = 0.1418) didn't reveal statistically significant differences in locality-specific burden between PBS- and AG-treated groups.

In this experiment, sera nitrite/nitrate levels were also measured using Griess reaction to test the effect of AG on an organismal scale. The results show similar trend as shown in Figure 2 and the results are presented in Figure S2.

4.1.3.3. MBP staining

MBP was detected in the subset of schistosomula-positive slides to assess nervous tissue demyelination. MBP signal was equally distributed in all examined slides of both control and AG-treated mice at 0, 7 and 14 dpi, no signs of demyelination were noticed (representative pictures are shown in Figure 12). Neither numerical analysis of the captured images revealed any significant differences in MFI of MBP signal (see Figure 13) (two-way ANOVA with Sidak's multiple comparisons test of log-transformed values to reach normality; time: $F(2, 85) = 0.6959$, $P = 0.5014$; treatment: $F(1, 85) = 0.6059$, $P = 0.4385$).

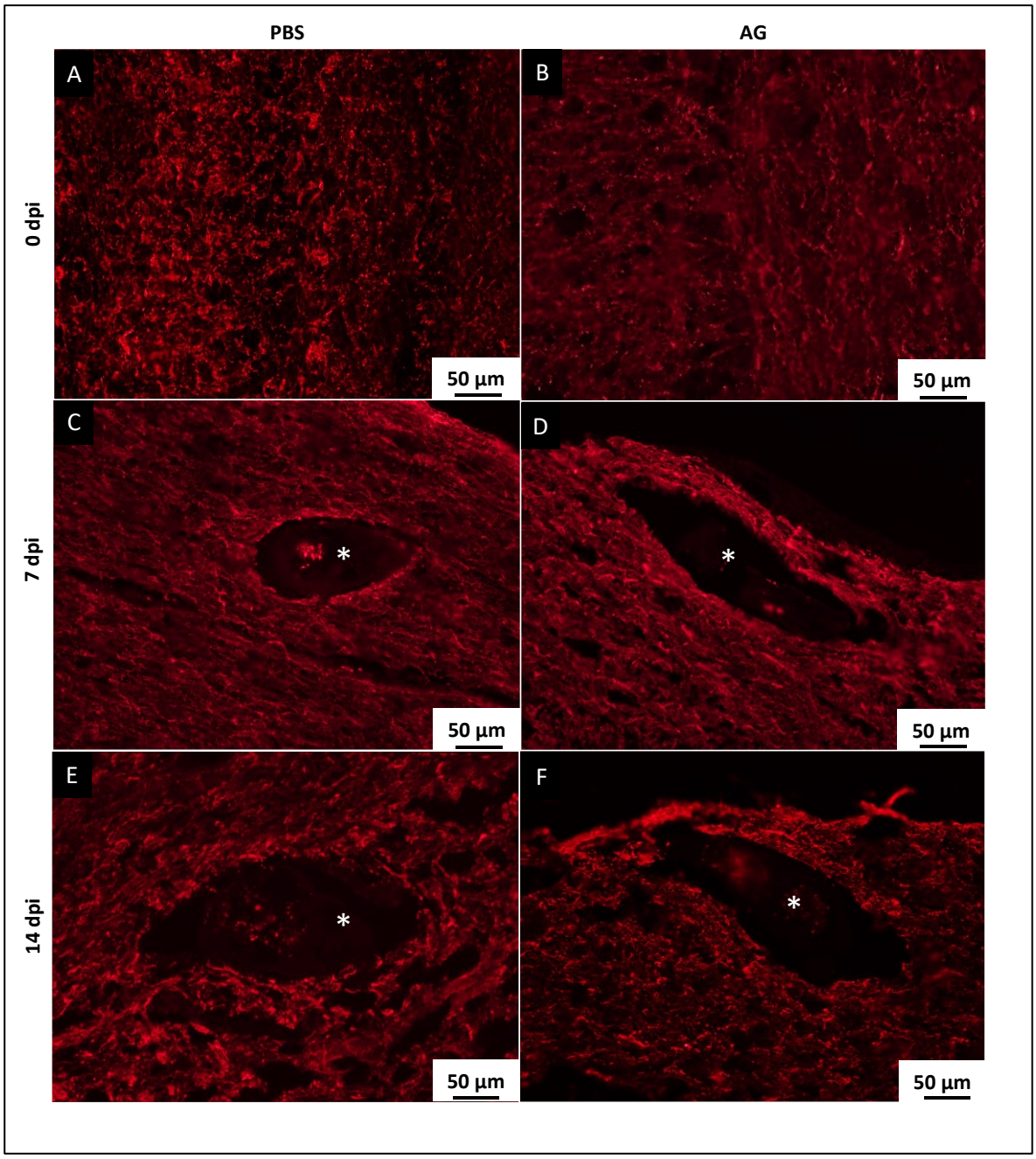

Figure 12: Representative pictures of MBP (red) staining in the infected spinal cord from mice injected with PBS (left column) or AG (right column) at 0 (A, B), 7 (C, D) and 14 (E, F) dpi. n (0 dpi) = 2 mice per group; n (7; 14 dpi) = 3 mice per group. Abbreviations: MBP – myelin basic protein; dpi – days post infection; * - schistosomulum *T. regenti* (the positive signal inside the worm represents ingested myelin positive for MBP)

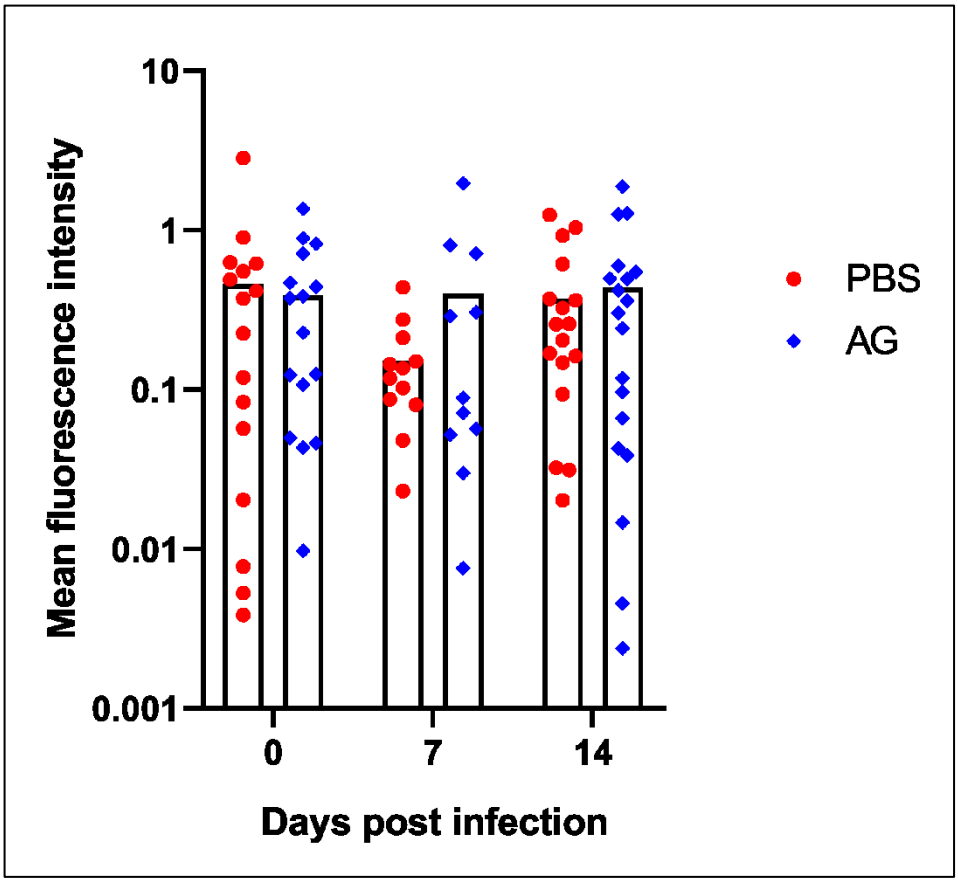

Figure 13: Summary of MFI obtained from normalized pictures of MBP signal in infected spinal cords with PBS- (red) or AG-injections (blue) at 0 (n = 2 mice per group), 7 (n = 3 mice per group) and 14 (n = mice per group) dpi. At least 3 schistosomula-positive slides per mouse were examined. Data are presented as mean and individual values (i. e. schistosomula-positive slides). MFI is shown in a logarithmic scale. Two-way ANOVA with Sidak's multiple comparisons test didn't show any significant differences in MFI either between PBS- and AG-treated groups or during infection. Abbreviations: MFI – mean fluorescence intensity; MBP – myelin basic protein; dpi – days post infection.

4.2. *In vitro* experiments

4.2.1. Viability measurement after SIN-1 treatment

Two approaches were used to assess schistosomula viability after their 48-hour treatment with 1.5 and 3.0 mM SIN-1, the peroxynitrite donor. The control group (0 mM SIN-1) was left in the medium only. For each group, 4×30 schistosomula were used and the experiment was repeated 3 times. Lactate levels were highest in the media from the control group and the group treated with 1.5 mM SIN-1, whereas significantly less lactate ($P = 0.0001$) was measured in 3 mM SIN-1 treated group (Figure 14A) (one-way ANOVA with Dunnett's multiple comparisons test performed on log-transformed values, $F(4,41) = 252.6$).

In case of methylene blue dye, schistosomula were considered dead when they were medium to dark blue. The percentage of methylene-blue unstained schistosomula was significantly higher in the control group compared to both 1.5 and 3.0 mM SIN-1 treated groups (Figure 14B) (one-way ANOVA with Dunnett's multiple comparisons test, $F(2, 9) = 205.6$; $P = 0.0001$).

4.2.2. SEM imaging of schistosomula after SIN-1 treatment

All control schistosomula (11 examined individuals) had tegument with fully developed spines and pouches (Figure 15A, B). Tegumental spines and pouches of schistosomula cultivated with 1.5 mM SIN-1 (7 examined individuals) were less frequent than in control ones and in some cases, holes were formed in the tegument (Figure 15C, D). The tegument of schistosomula cultivated with 3.0 mM SIN-1 (6 examined individuals) was underdeveloped with little spines or pouches, cracked and in many cases, partially or completely peeled off (Figure 15E-H).

4.2.3. TEM imaging of schistosomula after SIN-1 treatment

The tegument structure was virtually similar in control schistosomula (6 examined individuals) and those treated with 1.5 mM SIN-1 (10 examined individuals) (Figure 16A-D) showing no pathological alterations. The same was true for subtegumental cells, muscle fibers and mitochondria. On the other hand, the integrity of tegument and mitochondria in muscle cells was impaired in schistosomula cultivated with 3 mM SIN-1 (7 examined individuals). Tegument was peeled off (Figure 16E) and mitochondria were swollen without clearly defined cristate (Figure 16F).

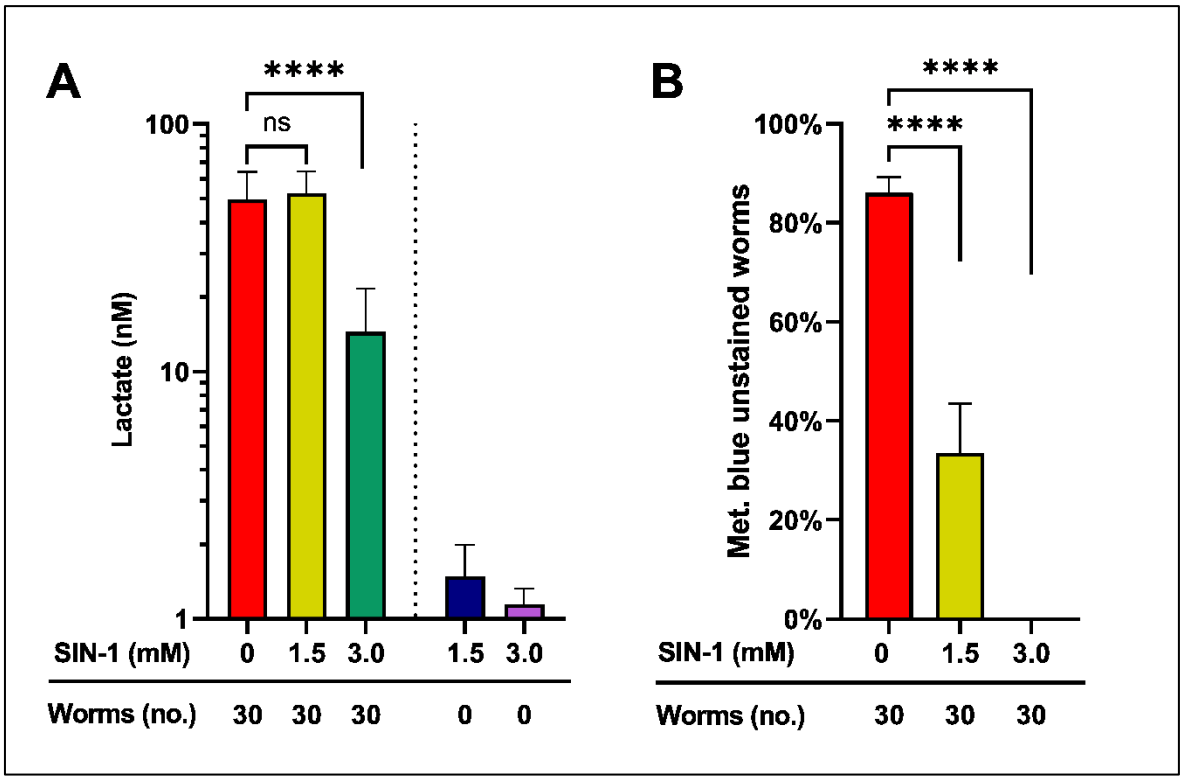

Figure 14: Examination of schistosomula viability after 48-hour treatment with SIN-1, the peroxynitrite donor, using measurement of lactate production (A) and methylene blue staining (B). Schistosomula (30 per well, 4 wells per group, 3 repetitions) were cultivated with 1.5 or 3.0 mM SIN-1 and lactate levels were measured in cultivation media (A, data shown in logarithmic scale). Schistosomula cultivated without SIN-1 (30 per well, 4 wells) and SIN-1 itself (in corresponding concentrations) were used as controls. Cultivated schistosomula were then stained with methylene blue. Percentage of unstained (living), schistosomula is shown in B. ANOVA showed significant differences between 3.0 mM SIN-1 group and control groups in both methods. In case of methylene blue, significant difference between 1.5 mM SIN-1 and control groups was also shown. Data are shown as means ± SD.

Figure 15 (see page 46): Representative SEM images of schistosomula after 48-hour treatment with SIN-1. A-B: *Control (untreated) schistosomulum (A) and detail of the well-developed tegument with spines (sp) and pouches (po).* C-D: *Schistosomulum treated with 1.5 mM SIN-1 (C) and detail of the underdeveloped tegument with holes (ho), less spines and pouches than present on the surface of control schistosomula.* E-H: *Schistosomulum treated with 3.0 mM SIN-1 (E) and details of the tegument peeling off the schistosomulum (F, G) and the remaining "naked" surface of basal lamina (H).*

Figure 16 (see page 47): Representative TEM images of schistosomula cultivated with 3 mM SIN-1 (7 examined individuals) (A, B), 1.5 mM SIN-1 (10 examined individuals) (C, D) and control schistosomula (6 examined individuals) (E, F). A: *intact control schistosomulum with tegument with spines and healthy mitochondria*; B: *intact mitochondria*; C: *intact 1.5 mM SIN-1-treated schistosomulum with tegument with spines and intact musculature*; D: *intact mitochondria*; E: *tegument peeling off schistosomulum*; F: *schistosomulum without tegument with damaged mitochondria*. Abbreviations: T – tegument; s – spines; lb – lamina basalis; mu – muscle; fc – flame cell; * - mitochondria

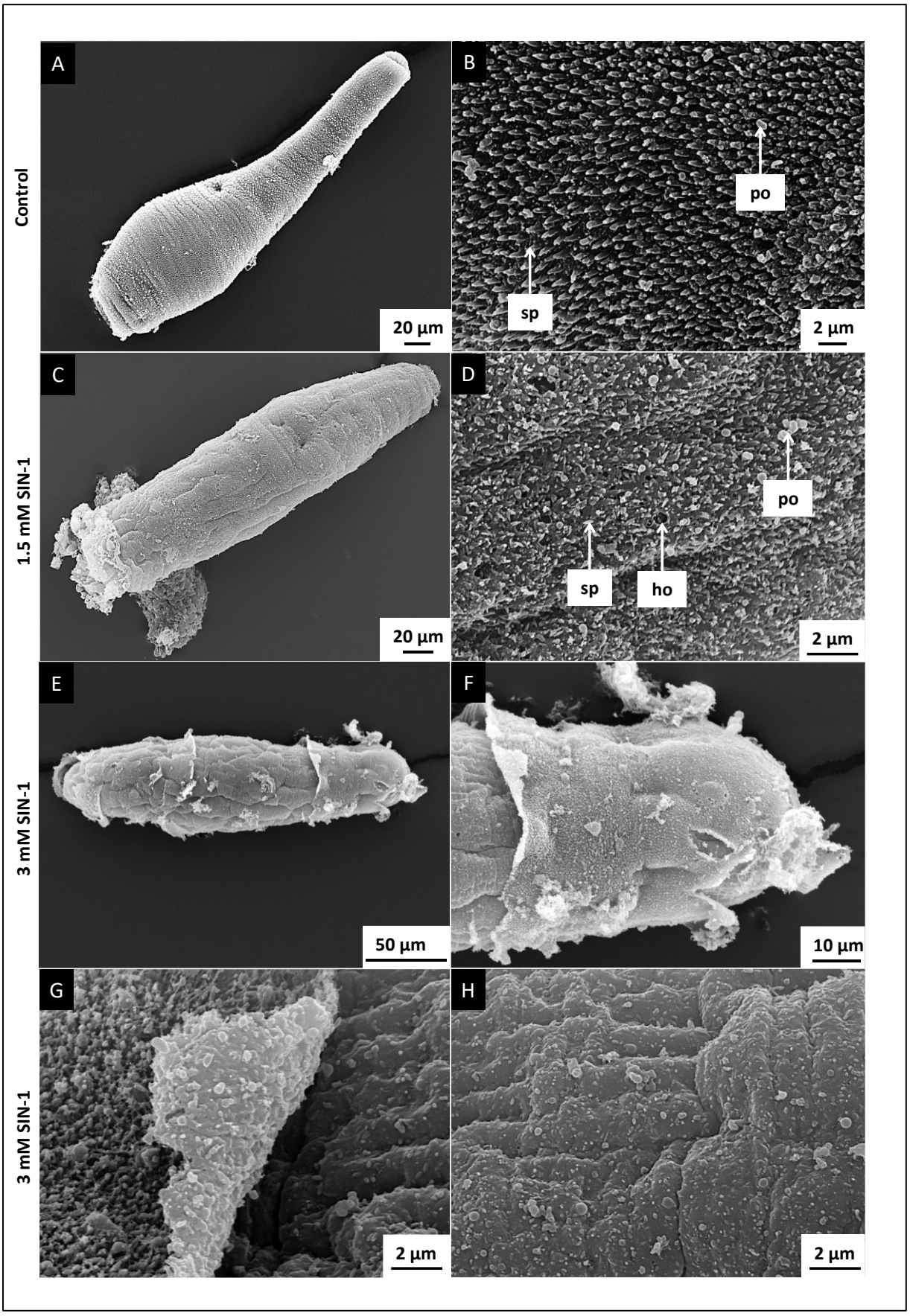

Figure 15: Representative SEM images of control schistosomula (A, B) and schistosomula cultivated with 1.5 mM (C, D) and 3 mM (E, F, G, H) SIN-1. For further description see page 45.

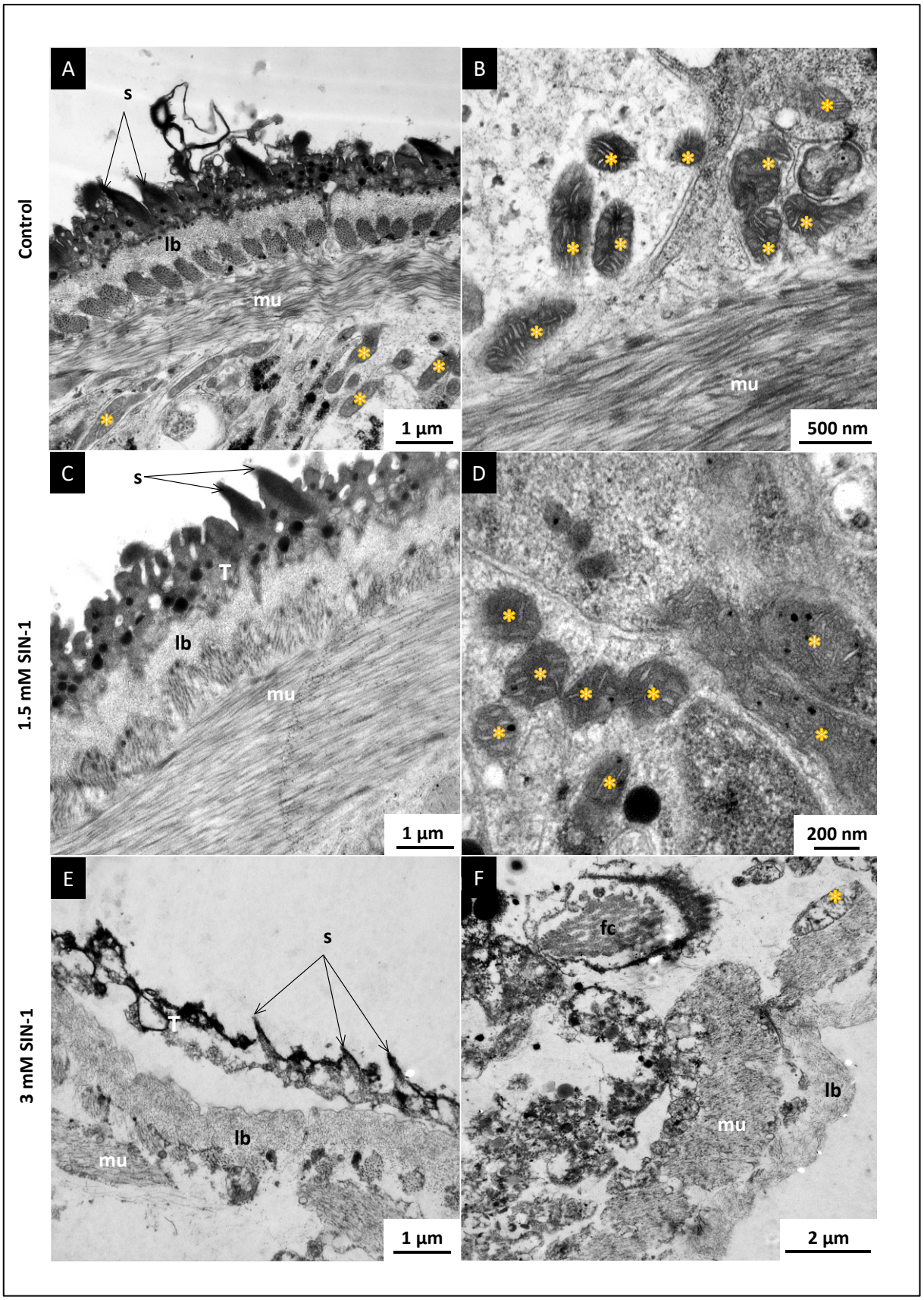

Figure 16: Representative TEM images of control schistosomula (A, B) and schistosomula cultivated with 1.5 mM (C, D) and 3 mM (E, F) SIN-1. For further description see page 45.

5. Discussion

Penetration of mammalian skin by *T. regenti* triggers immune response represented by neutrophils, eosinophils and macrophages, which infiltrate the penetration site within 24 hours (Kouřilová et al., 2004b). During the next migration through nerves and the spinal cord, the schistosomula cause axonal damage and attract, besides afore mentioned cells, also immune cells specific for CNS – microglia and astrocytes (Kouřilová et al., 2004b; Lichtenbergová et al., 2011). Even though the presence of immune cells correlates with observed damage to schistosomula (Lichtenbergová et al., 2011), little is known about the effector molecules responsible for elimination of the migrating schistosomula. In case of human schistosomes, NO was shown to have strong anti-parasitic effects impairing parasite development and growth, which led to reduction of liver pathology (Shen et al., 2017). Given that all immune cells attracted to *T. regenti* schistosomula (macrophages, neutrophils, eosinophils, microglia and astrocytes) are capable of iNOS synthesis, the role of NO during *T. regenti* infections examined in this thesis applying both *in vivo* and *in vitro* approaches.

On an organismal level, NO production during infection can be indirectly detected by measuring nitrites/nitrates in serum or urine. In our experiment, intraperitoneal LPS injections significantly increased nitrite/nitrate levels in sera of tested animals. It demonstrates if the nitrite/nitrate levels would rise after *T. regenti* infections, we would be able to detect it. Elevated nitrite/nitrate levels in sera from infected animals were described in monkeys with chronic *T. cruzi* infection with confirmed iNOS synthesis in the heart (Marcelo et al., 2012) but no significant increase was observed in sera obtained from C57BL6/J infected with *Clonorchis sinensis* (Yang et al., 2017). To our knowledge, NO was not measured on a systemic scale during schistosomosis or any parasitosis affecting CNS giving us no relevant results for comparison. Nevertheless, our results show that, unlike LPS injections, *T. regenti* infections did not cause a rise in serum nitrite/nitrate levels in our experimental animals suggesting that *T. regenti* infection does not stimulate NO production enough to be detectable on a systemic scale. Based on that, it was expected that AG would not cause significant changes in nitrite/nitrate levels in the sera, which was experimentally confirmed.

When we examined NO production more closely, meaning at the specific infection sites (mouse pinnae and spinal cords) we observed iNOS signal in infected pinnae at 8 hpi when neutrophils, but not yet eosinophils and macrophages, are present in the infection site (Kouřilová et al., 2004b). Similar composition of cells migrating to the infected tissue was also described in *S. mansoni* infections (Ch'ang and Colley, 1986) and iNOS synthesis was described in schistosome infections at 24 hpi (Ramaswamy et al., 1997). Produced NO then protected the host and reduced parasite load

in *S. japonicum* infections (Liu et al., 2015). Neutrophils migrating to the *T. regenti* infection site might produce NO with similar host-protective effect. Nevertheless, the observed distribution of the iNOS signal in the upper skin layers led us to believe that rather keratinocytes are the iNOS producing cells in *T. regenti* infections. Keratinocytes were proved to produce iNOS in case of skin injuries (Frank et al., 1998) and NO presence in the injured skin improved the healing process by inducing keratinocyte proliferation and VEGF production (Frank et al., 2002). NO was also proved to be one of the effectors accelerating healing of leishmania-caused ulcers (Miranda et al., 2015). We therefore hypothesize that NO production in the skin during *T. regenti* infection is driven rather by the parasite-driven skin injury than by parasite presence. Unfortunately, 3-NT presence could not have been tested as we ran out of primary antibody, therefore we were not able to establish if NO could also have some negative impact on parasite itself. Moreover, we did not expect 3-NT signal at chosen timepoints as we observed 3-NT in the spinal cord in the later phase of the infection. We therefore suggest repeating the experiment using later timepoints. If NO had negative impact on parasites in the skin, 3-NT would probably be detected later in the tissue surrounding the parasite as well as in the parasite itself.

After the skin penetration, schistosomula migrate to the spinal cords where the resident immune cells, astrocytes and microglia, are capable of iNOS expression (Simmons and Murphy, 1992). Soluble fraction of *T. regenti* schistosomula homogenate was proved to activate NO production by astrocytes and microglia *in vitro* (Macháček et al., 2016) therefore iNOS presence was examined in the infected spinal cord *in vivo* in this study. We observed iNOS signal at 3 dpi (and once at 7 dpi) and not in the later signal. Therefore, we believe that the observed signal is really iNOS and not an artefact of schistosomula metabolism (meaning that the antibody would non-specifically bind to some products of the parasite). If that was the case, the signal would be present throughout the whole infection. In the muscle phase of *T. spiralis* infection, iNOS was detected in eosinophil-deficient mice in close proximity to the parasite (Fabre et al., 2009), similarly to our results. The authors hypothesize that in *T. spiralis* infection, classically activated macrophages were responsible for NO production and parasite destruction (Fabre et al., 2009). As microglia and astrocytes are the resident immune cells in the spinal cord, we decided to examine if astrocytes or microglia produce NO *in vivo* by colocalization of iNOS signal with their cellular markers. Unfortunately, our colocalization analysis didn't show that these cells would be the ones producing NO *in vivo*. That is in accordance with in vitro results, which showed that astrocytes managed to kill schistosomula but did not produce nitric oxide (Macháček et al., 2016). Nevertheless, immune cells infiltrating the spinal cord (macrophages or neutrophils) (Kouřilová et al., 2004b; Lichtenbergová et al., 2011) might be the ones responsible for NO production. Eosinophils are not believed to produce NO as

they participate in dampening of Th1 response with NO production in *T. spiralis* infections (Fabre et al., 2009). To examine which cells produce NO in the *T. regenti* infected spinal cord, one of two experiments should be performed. First would be IHC colocalization analysis, similar to the one performed on astrocytes and microglia, using different cellular markers specific for myeloid cells. Second would be flow cytometry carried out on cells from infected spinal cord marked for iNOS and myeloid cells; alternatively, fluorogenic probes can be used as well during flow cytometry to detect NO. The latter experiment employing flow cytometry is expected to be more specific and therefore should be preferred in further experiments.

NO production during *T. regenti* infection was further confirmed by 3-NT detection in the infected spinal cords at 7, 14 and 21 dpi. 3-NT was also detected in neurons in *T. cruzi* infected mice, specifically in the neuronal cytoplasm (Bombeiro et al., 2010). On the other hand, our 3-NT signal appeared to at least partially colocalize with DAPI signal from nuclei rather than be dispersed in the cytoplasm. Nevertheless, our signal was visually comparable with 3-NT signal detected in inflamed murine liver and human colon samples (Wisastra et al., 2011) suggesting that we indeed detected 3-NT in the *T. regenti* infected spinal cord. Further colocalization analysis using confocal microscopy revealed that 3-NT and DAPI signals seem to complete each other rather than overlap suggesting that 3-NT is not formed directly on the nuclear lamina.

The time difference between the appearance of iNOS and 3-NT was rather peculiar, given that 3-NT formation can be detected within hours after injury in plant cells (Romero-Puertas et al., 2008), which, unlike animal cells, have extra protection in form of cell wall. Unfortunately, we were only able to find information that 3-NT is a stable end product of RNS-caused nitrosylation (Crowley et al., 1998; Hess et al., 2005; Tsikas and Duncan, 2014) without specific turnover time. However, we consider it unlikely that RNS, either NO or peroxynitrite, would circulate in the surrounding tissue for as long as 18 days, therefore other NOS were taken into the account. It was described that CNS injury leads to local rise in Ca^{2+} levels (Decoster, 1995) which would then lead to higher nNOS activity in the schistosomula-injured area and more detected 3-NT in the later phases of the infection. The distance between nNOS and the targeted protein correlates with specificity of NO-induced nitrosylation (Hess et al., 2005) which would explain why the 3-NT was detected in the cells within and around the injury but not in such close proximity to the worm as iNOS. The hypothesis that NO produced by NOS different than iNOS is responsible for 3-NT formation might be tested by IHC staining of nNOS or on $iNOS^{-/-}$ mice. If 3-NT would still be present in the infected $iNOS^{-/-}$ spinal cords, it would confirm our hypothesis.

The results from the experiments described above have shown that *T. regenti* stimulates NO production in infected mice, both in the affected skin and spinal cord. Said NO production cannot be detected on the systemic scale, nevertheless, we have confirmed that NO is produced both in the entry site and in the migratory route by IHC staining for iNOS and 3-NT. Nevertheless, described experiments have not explored the NO effect on damage associated with immune response to the infection and parasite burden.

NO presence in the spinal cord could negatively affect not only parasites but also the tissue itself. NO production in the spinal cord can lead to neuronal death (Dawson and Dawson, 2018; Stewart et al., 2002) and has been associated with neurodegeneration in mice infected with *T. cruzi* (Bombeiro et al., 2010). To be more specific, NO produced by activated macrophages proved to block axonal conduction (Shrager and Youngman, 2017), cause axon breaks and axonal swelling (Venkataramana et al., 2015) damage neuronal mitochondria which lead to axonal damage resulting in demyelination during leprosy (Madigan et al., 2017). Demyelination was also described in neurotoxocarosis (Heuer et al., 2015; Springer et al., 2019). Nevertheless, even though *T. regenti* schistosomula cause axonal damage as they migrate through the spinal cord, it seems that they do not cause demyelination of the infected tissue (Lichtenbergová et al., 2011). Here, we focused on the effect of NO depletion by AG treatment on the levels of MBP, essential part of the myelin (Boggs, 2006). We did not observe any visible changes in MBP staining of the spinal cord after the infection and according to our results, AG did not cause any changes in MBP staining. To confirm IHC results, MFI from MBP signal were extracted and compared revealing no significant changes in MBP levels. We therefore concluded that neither *T. regenti* infections nor NO production affect myelination in the spinal cord nervous tissue. Nevertheless, NO could affect nervous tissue differently than by demyelination, for example by triggering cell apoptosis. NO has been described as both pro- and anti-apoptotic, however, NO proapoptotic effects were linked to iNOS presence and pathology caused in site (Zhang et al., 2017). NO has also been known for causing neutrophil apoptosis (Dubey et al., 2016) which are the first responding immune cells in the *T. regenti* infected spinal cords (Kouřilová et al., 2004b). Taken together, NO produced in reaction to the infection might, rather than cause demyelination, ignite the apoptosis of many cells surrounding the schistosomula in the spinal cord which could then be detected for example by TUNEL assay.

Experiments comparing parasite burden in the AG-treated and non-treated animals showed that iNOS inhibition by AG led to higher burden in animals infected with *S. mansoni* (Wynn et al., 1994), *B. malayi* (Rajan et al., 1996) and *S. venezuelensis* (Ruano et al., 2015) suggesting the positive role of RNS in control of the infection. In case of *T. regenti* infections, AG-induced iNOS inhibition did not have significant effect on parasite burden or schistosomula distribution within the infected

spinal cord. Regardless, less schistosomula were found in the spinal cords retrieved from AG-treated mice than from control mice, albeit the difference was not significant. These results suggest a trend opposite to the afore mentioned cases, where NO decreased the parasite burden. We were unable to confirm or disprove this trend because only 3 mice per group were used in our experiment. If the repetition of this experiment would confirm the AG-induced trend, it would suggest that different, possibly Th2 related molecules are important for parasite clearance. In neurocysticercosis caused by *M. corti*, Th2-related alternatively activated macrophages were described as effective in parasite clearance (Mishra et al., 2012). Th2-related cytokines (IL-4, IL-5, IL-9, IL-13) proved to efficiently protect intestine from parasites (Cortés et al., 2017). One of the mentioned cytokines, IL-4, was also described in the spinal cord in the later phases of *T. regenti* infection (Majer, 2018) and macrophages, without the specification of the activation, were described as one of the cells migrating to the infected spinal cord (Kouřilová et al., 2004b; Lichtenbergová et al., 2011). Taken together, it is possible that RNS start the parasite destruction but, later in the infection, alternatively activated macrophages together with Th2-related cytokines are necessary for *T. regenti* clearance.

Given that CNS has long been considered immunoprivileged site, one might object that AG does not affect the course of *T. regenti* infection simply because it is not capable of crossing the blood-brain barrier (BBB). However, lymphatic system surrounding the dura mater can drain even immune cells from the tissue (Negi and Das, 2018). As for the molecules crossing the BBB, their size varies from small minocycline (Shultz and Zhong, 2017) to larger amyloid-β (Louveau et al., 2017) suggesting that AG, smaller than minocycline, should be able to cross the BBB and inhibit NO production in the spinal cord.

Last explanation as to why AG did not cause any significant differences in the course of infection presents itself after looking at the preliminary results. Particularly, AG was not able to reduce nitrite/nitrate levels in the sera to control levels. Used concentration and mode of administration, 50 mg/kg i.p., significantly reduced parasite burden in *T. spiralis* infections (Kołodziej-Sobocińska et al., 2006) suggesting that if NO would affect parasite burden, we would be able to detect it. However, AG administered in said concentration inhibits approximately 70% of LPS-induced elevation in nitrite/nitrate levels in murine sera (Tracey et al., 1995) and this imperfect inhibition might cause the insignificant differences in parasite burden as residual NO production might be sufficient for maintaining the balance in the efficient immune response. To properly explore iNOS inhibition, we suggest using iNOS$^{-/-}$ mice and compare the course of infection in iNOS$^{-/-}$ and WT mice. Adding IHC and flow cytometry analysis of Th2 response to this experiment would clarify the role of NO as well as point to Th2-related cells and effectors responsible for parasite clearance.

While we were able to confirm NO production after the infection, AG inhibition of NO production did not reveal any significant differences in the parasite burden and myelination. Nevertheless, the *in vivo* experiments did not explore the effect of RNS on parasite itself. To further and closely explore the effect of RNS, we implemented *in vitro* experiments as well with focus on schistosomula viability and ultrastructure.

According to literature, macrophages cultivated with S. mansoni schistosomula significantly reduced parasite viability (James and Glaven, 1989). The authors of the study hypothesize that NO is responsible for the effect. Nevertheless, adding NOR-5, NO donor, to the manually transformed *T. regenti* schistosomula did not increase mortality rate in the culture (Pankrác and Macháček, 2017) suggesting no toxic effect of NO on schistosomula. This could have three explanations. Firstly, it is possible that RNS altogether do not affect *T. regenti* schistosomula viability. Secondly, it is possible that not NO but peroxynitrite, result of presence of both RNS and ROS which was also proved to kill *Fasciola* adults (Sadeghi-Hashjin and Naem, 2001), might affect *T. regenti* schistosomula viability. Thirdly, it is possible that RNS affect schistosomula viability but the method chosen for assessing schistosomula viability (methylene blue staining) might have not been optimal. To be specific, methylene blue staining has two major disadvantages: it only recognizes unstained, viable schistosomula or blue, dead schistosomula (Li Hsü et al., 1977) and it is prone to researcher's bias as the level of staining is evaluated by eye. To rule out or confirm some of afore mentioned explanations, manually transformed schistosomula were cultivated with SIN-1, peroxynitrite donor, and different viability-assessing method was applied in this study.

In case of *S. mansoni*, lactate levels proved to reliably reflect schistosomula viability (Howe et al., 2015). Lactate is produced by organisms with anaerobic metabolism. Based on transcriptomic data, *T. regenti* schistosomula have microaerobic metabolism (Leontovyč et al., 2016) and should produce lactate as the end-product of glucose degradation. Therefore, lactate assay was chosen to test schistosomula viability after their incubation with SIN-1. Methylene blue staining was used for comparison. Lactate level measurement show that lower (1.5 mM) SIN-1 concentration did not affect metabolic functions of schistosomula. Higher (3 mM) SIN-1 concentration, on the other hand, significantly diminished schistosomula lactate metabolism and therefore their viability. Methylene blue supports viability assessment by lactate measurement in case of control group and 3 mM SIN-1 treated group. In case of 1.5 mM SIN-1 treated schistosomula, methylene blue dye showed higher schistosomula mortality rate than lactate levels. If lower concentration of peroxynitrite only affected tegument which then died and methylene blue was able to stain it, such schistosomula would seem dead to the researcher's eye even though the schistosomula would still be metabolically active, therefore alive. This experiment demonstrated the disadvantages of

methylene blue staining, proved that lactate levels reflect *T. regenti* schistosomula viability and, most importantly, showed that peroxynitrite negatively affects schistosomula viability.

Peroxynitrite caused severe changes in the schistosomula ultrastructure with striking differences in tegumental architecture. Control (untreated) schistosomula had developed tegument with spines and pouches and intact parenchyma and mitochondria with well-defined cristae. Schistosomula cultivated with lower concentration of peroxynitrite revealed teguments with holes and less spines under SEM, but under TEM these schistosomula appeared intact and the same as control schistosomula. Neither closer examination with focus on tegument, namely on membrane detachment, vacuolation, density of tegumental spherical bodies and on appearance of mitochondria and myofilaments in muscles, revealed significant changes in the ultrastructure. The results from EM seem to prove our hypothesis that lower concentration of peroxynitrite causes only mild surface changes, possibly leading to changes in membrane permeability resulting in seemingly blue schistosomula, but does not affect vital organelles. Treatment with higher concentration of peroxynitrite, on the other hand, led to smaller number of spines, perforated tegument ultimately peeling off of schistosomula, changes to parenchyma structure and disintegration of mitochondrial cristae. The mitochondrial damage and parenchymal alterations were also described in schistosomula cultivated with activated macrophages (presumably producing RNS and ROS) while tegument remained intact (McLaren and James, 1985). Changes in mitochondria were also described in *S. japonicum* adults retrieved from rats producing high levels of NO and efficiently reducing parasite burden (Shen et al., 2017). As for the tegument, changes similar to the ones we have observed (smaller number of spines, tegument peeling off) were also observed in adults of *S. haematobium* killed by artemisin-based compound (El-Beshbishi et al., 2018) and in *S. mansoni* and *S. haematobium* adults killed by curcumin (Abou El Dahab et al., 2019). Moreover, similar loss of spines and tegument peeling off was also described in adults retrieved from animals treated with PZQ, drug used for treating schistosomosis (Shaw and Erasmus, 1987). Peroxynitrite therefore appears to affect *T. regenti* schistosomula in the same way as NO and drugs affect human schistosomes. Nevertheless, the exact effect of peroxynitrite when first tegument and then mitochondria are damage remains unclear. The hypothesis for PZQ effect on *S. mansoni* adults, proposed by Shaw and Erasmus (1987), seems to fit the peroxynitrite effect on *T. regenti* schistosomula quite well. The authors attribute the tegumental changes to irreversible changes to cell physiology due to PZQ which then lead to the inability of tegument repair (Shaw and Erasmus, 1987). It is possible that NO irreversibly changes the cell homeostasis leaving tegument without the chance to be repaired, which would explain the phenomenon observed in schistosomula cultivated

with smaller concentration of peroxynitrite, later causing its peeling off and ultimately damages mitochondria causing cell death.

Given that higher concentration of peroxynitrite causes similar ultrastructural changes as drugs and compounds proved to efficiently terminate schistosomes, we hypothesize that peroxynitrite might be one of the molecules negatively influencing the viability of *T. regenti* schistosomula *in vivo*. We demonstrated that NO is produced at infection sites where ROS are presumably (due to proinflammatory cytokine milieu) present as well enabling formation of peroxynitrite. Nevertheless, given that lower concentration of peroxynitrite did not cause significant changes in schistosomula viability and ultrastructure and that iNOS inhibition, which would result in lower levels of peroxynitrite as well, did not significantly alter the course of *T. regenti* infection, peroxynitrite is unlikely to be the main molecule responsible for parasite clearance leaving the hunt for this molecule(s) open for future experiments.

6. Conclusion

NO is an effector molecule efficient in eliminating parasites from mammalian hosts. However, its role in clearance of *T. regenti* infection in accidental hosts has not been explored yet. Therefore, NO production in the accidental hosts of *T. regenti*, C57BL/6J mice, was examined as well as the changes in the course of infection and worm burden in mice with diminished NO production. Furthermore, the effect of peroxynitrite on mechanically transformed schistosomula was evaluated.

The main results of this thesis are:

- On a systemic level, the concentration of nitrites/nitrates (oxidation products of NO) in murine sera did not significantly change during *T. regenti* infections suggesting that the infection does not stimulate a systemic NO production.
- NO production was confirmed in the early phase of the infection in close proximity to schistosomula in the skin and spinal cord using IHC staining of iNOS showing that *T. regenti* triggers local NO production.
- Nitrosylated proteins (3-NT) were detected in the later phase of the infection in the spinal cord suggesting that other NO synthases might be more active during the infection as well.
- Inhibition of NO production did not significantly the parasite burden in spinal cords and the amount of myelin basic protein in affected areas. It suggests that other mechanisms than NO production are responsible for parasite clearance in the later phase and that NO does not cause demyelination.
- Peroxynitrite negatively affected schistosomula viability, as well as the integrity of schistosomula tegument suggesting that peroxynitrite might be one of the molecules protecting the host from the infection.

The results of this study widened the knowledge of immune reaction of *T. regenti* infected mice with respect to NO, a part of innate immune system. It will serve as a starting point for more thorough investigation of the role of the innate immune mechanisms in the regulation of *T. regenti* infection in mice.

References

Abou El Dahab, M.M., Shahat, S.M., Mahmoud, S.S.M., and Mahana, N.A. (2019). In vitro effect of curcumin on Schistosoma species viability, tegument ultrastructure and egg hatchability. Exp. Parasitol. *199*, 1–8.

Ahmed, F.S., Oswald, I.P., Caspar, P., Hieny, S., Keefer, L., Sher, A., and James, S.L. (1997). Developmental differences determine larval susceptibility to nitric oxide-mediated killing in a murine model of vaccination against Schistosoma mansoni. Infect. Immun. *65*, 219–226.

Alonso-Trujillo, J., Rivera-Montoya, I., Rodríguez-Sosa, M., and Terrazas, L.I. (2007). Nitric oxide contributes to host resistance against experimental Taenia crassiceps cysticercosis. Parasitol. Res. *100*, 1341–1350.

Amri, M., and Touil-Boukoffa, C. (2015). A protective effect of the laminated layer on Echinococcus granulosus survival dependent on upregulation of host arginase. Acta Trop. *149*, 186–194.

Amri, M., Aissa, S.A., Belguendouz, H., Mezioug, D., and Touil-Boukoffa, C. (2007). In vitro antihydatic action of IFN-gamma is dependent on the nitric oxide pathway. J. Interferon Cytokine Res. *27*, 781–787.

Andrade, M.A., Siles-Lucas, M., López-Abán, J., Nogal-Ruiz, J.J., Pérez-Arellano, J.L., Martínez-Fernández, A.R., and Muro, A. (2007). Trichinella: Differing effects of antigens from encapsulated and non-encapsulated species on in vitro nitric oxide production. Vet. Parasitol. *143*, 86–90.

Asensio, V.C., Oshima, H., and Falanga, B.P. (1993). Plasmodium berghei: Is nitric oxide involved in the pathogenesis of mouse cerebral malaria? Exp. Parasitol. *77*, 111–117.

Beckman, J.S., and Koppenol, W.H. (1996). Nitric oxide, superoxide, and peroxynitrite: the good, the bad, and the ugly. Am. J. Physiol. Regul. Integr. Comp. Physiol. *271*, C1424-1437.

Beckman, J.S., Chen, J., Woerd, V. Der, Zhu, L., Martin, J.C., and Smith, C. (1992). Kinetics of superoxide dismutase and iron-catalyzed nitration of phenolics by peroxynitrite. Arch. Biochem. *298*.

Bian, K., Harari, Y., Zhong, M., Lai, M., Castro, G., Weisbrodt, N., and Murad, F. (2001). Down-regulation of inducible nitric-oxide synthase (NOS-2) during parasite-induced gut inflammation: a path to identify a selective NOS-2 inhibitor. Mol. Pharmacol. *59*, 939–947.

Bogdan, C. (2001). Nitric oxide and the immune response. Nat. Immunol. *2*, 907–916.

Bogdan, C., Röllinghoff, M., and Diefenbach, A. (2000). Reactive oxygen and reactive nitrogen intermediates in innate and specific immunity. Curr. Opin. Immunol. *12*, 64–76.

Boggs, J.M. (2006). Myelin basic protein: A multifunctional protein. Cell. Mol. Life Sci. *63*, 1945–1961.

Bombeiro, A.L., D'Império Lima, M.R., Chadi, G., and Álvarez, J.M. (2010). Neurodegeneration and increased production of nitrotyrosine, nitric oxide synthase, ifn-γ and s100β protein in the spinal cord of il-12p40-deficient mice infected with trypanosoma cruzi. Neuroimmunomodulation *17*, 67–78.

Brunet, L.R. (2001). Nitric oxide in parasitic infections. Int. Immunopharmacol. *1*, 1457–1467.

Brunet, L.R., Beall, M., Dunne, D.W., and Pearce, E.J. (1999). Nitric oxide and the Th2 response combine to prevent severe hepatic damage during Schistosoma mansoni infection. J. Immunol. *163*, 4976–4984.

Bulantová, J., Macháček, T., Panská, L., Krejčí, F., Karch, J., Jährling, N., Saghafi, S., Dodt, H.U., and Horák, P. (2016). Trichobilharzia regenti (Schistosomatidae): 3D imaging techniques in characterization of larval migration through the CNS of vertebrates. Micron *83*, 62–71.

Ch'ang, L.-Y., and Colley, D.G. (1986). Cutaneous Sensitivity Induced by Immunization with Irradiated Schistosoma mansoni Cercariae. Cell. Immunol. *100*, 119–128.

Chanová, M., Bulantová, J., Máslo, P., and Horák, P. (2009). In vitro cultivation of early schistosomula of nasal and visceral bird schistosomes (Trichobilharzia spp., Schistosomatidae). Parasitol. Res. *104*, 1445–1452.

Cleeter, M.W.J., Cooper, J.M., Darley-Usmar, V.M., Moncada, S., and Schapira, A.H. V (1994). Reversible inhibition of cytochrome c oxidase, the terminal enzyme of the mitochondrial respiratory chain, by nitric oxide: implications for neurodegenerative diseases. FEBS Lett. *345*, 50–54.

Cortés, A., Muñoz-antoli, C., Esteban, J.G., and Toledo, R. (2017). Th2 and Th1 Responses : Clear and Hidden Sides of Immunity Against Intestinal Helminths. Trends Parasitol. *33*, 678–693.

Coulson, P.S., Smythies, L.E., Betts, C., Mabbott, N.A., Sternberg, J.M., Wei, X.G., Liew, F.Y., and Wilson, R.A. (1998). Nitric oxide produced in the lungs of mice immunized with the radiation-attenuated schistosome vaccine is not the major agent causing challenge parasite elimination. Immunology *93*, 55–63.

Crowley, J.R., Yarasheski, K., Leeuwenburgh, C., Turk, J., and Heinecke, J.W. (1998). Isotope Dilution

Mass Spectrometric Quantification of 3-Nitrotyrosine in Proteins and Tissues Is Facilitated by Reduction to 3-Aminotyrosine. *135*, 127–135.

Curran, B.R.D., Billiar, T.R., Stuehr, D.J., Hofmann, K., and Simmons, R.L. (1989). Hepatocytes produce nitrogen oxides from L-arginine in response to inflammatory. *170*.

Dai, W.J., and Gottstein, B. (1999). Nitric oxide-mediated immunosuppression following murine Echinococcus multilocularis infection. 107–116.

Dai, W.E.N.J., Waldvogel, A., Siles-lucas, M.A.R., and Gottstein, B. (2004). Echinococcus multilocularis proliferation in mice and respective parasite 14-3-3 gene expression is mainly controlled by an αβ+ CD4+ T-cell-mediated immune response. Immunology 481–488.

Dai, W.J., Waldvogel, A., Jungi, T., Stettler, M., and Gottstein, B. (2003). Inducible nitric oxide synthase deficiency in mice increases resistance to chronic infection with Echinococcus multilocularis. *1*, 238–244.

Dawson, T.M., and Dawson, V.L. (2018). Nitric Oxide Signaling in Neurodegeneration and Cell Death (Elsevier Inc.).

Decoster, M.A. (1995). Calcium dynamics in the central nervous system. Adv. Neuroimmunol. *5*, 233–239.

Demirci, C., Gargili, A., Kandil, A., Cetinkaya, H., Uyaner, I., Boynuegri, B., and Koray Gumustas, M. (2006). Inhibition of inducible nitric oxide synthase in murine visceral larva migrans: Effects on lung and liver damage. Chin. J. Physiol. *49*, 326–334.

Dubey, M., Nagarkoti, S., Awasthi, D., Singh, A.K., Chandra, T., Kumaravelu, J., Barthwal, M.K., and Dikshit, M. (2016). Nitric oxide-mediated apoptosis of neutrophils through caspase-8 and caspase-3-dependent mechanism. Cell Death Dis. *7*, e2348-12.

El-Beshbishi, S.N., El Bardicy, S., Tadros, M., Ayoub, M., and Taman, A. (2018). Efficacy of artemisinin–naphthoquine phosphate against Schistosoma haematobium adult flukes: dose–effect relationship and tegumental alterations. J. Helminthol. 1–6.

Esparza, I., Mannel, D., Ruppel, A., Falk, W., and Krammer, P.H. (1987). Interferon γ and lymphotoxin or tumor necrosis factor act synergistically to induce macrophage killing of tumor cells and schistosomula of Schistosoma mansoni. Work *166*, 589–594.

Espinoza, E.Y., Pérez-arellano, J.L., Carranza, C., Collía, F., and Muro, A. (2002). In vivo inhibition of inducible nitric oxide synthase decreases lung injury induced by Toxocara canis in experimentally

infected rats. 511–520.

Fabre, V., Beiting, D.P., Bliss, S.K., Gebreselassie, N.G., Gagliardo, L.F., Lee, N.A., Lee, J.J., and Appleton, J.A. (2009). Eosinophil deficiency compromises parasite survival in chronic nematode infection. J. Immunol. *182*, 1577–1583.

Fang, F.C. (1997). Mechanisms of Nitric Oxide-related Antimicrobial Activity. J. Clin. Invest. *99*, 2818–2825.

Frank, S., Madlener, M., Pfeilschifter, J., Werner, S., Pharmakologie, Z. Der, and Goethe-universita, K.D.J.W. (1998). Induction of inducible nitric oxide synthase and its corresponding tetrahydrobiopterin-cofactor-synthesizing enzyme GTP-cyclohydrolase I during cutaneous wound repair. J. Invest. Dermatol. *111*, 1058–1064.

Frank, S., Kämpfer, H., Wetzler, C., and Pfeilschifter, J. (2002). Nitric oxide drives skin repair: Novel functions of an established mediator. Kidney Int. *61*, 882–888.

Garcia-Bonilla, L., Iadecola, C., Zhou, P., Racchumi, G., Moore, J.M., Butler, J.M., and Anrather, J. (2014). Inducible Nitric Oxide Synthase in Neutrophils and Endothelium Contributes to Ischemic Brain Injury in Mice. J. Immunol. *193*, 2531–2537.

Gargili, A., Demirci, C., Kandil, A., Çetinkaya, H., Atukeren, P., and Gümüştaş, M.K. (2004). In vivo inhibition of inducible nitric oxide and evaluation of the brain tissue damage induced by Toxocara canis larvae in experimentally infected mice. Chin. J. Physiol. *47*, 189–196.

Gray, C.A., and Lawrence, R.A. (2002). Interferon-γ and nitric oxide production are not required for the immune-mediated clearance of Brugia malayi microfilariae in mice. Parasite Immunol. *24*, 329–336.

Greenberg, S.S., Xie, J., Spitzer, J.J., Wang, J., Lancaster, J., Grisham, B., Powers, D.R., and Giles, T.D. (1995). Nitro containing L-arginine analogs interfere with assays for nitrate and nitrite. *57*, 1949–1961.

Guglielmo, S., Cortese, D., Vottero, F., Rolando, B., Kommer, V.P., Williams, D.L., Fruttero, R., and Gasco, A. (2014). New Praziquantel derivatives containing NO-donor furoxans and related furazans as active agents against Schistosoma mansoni. Eur J Med Chem *84*, 135–145.

Gupta, R., Bajpai, P., Tripathi, L.M., Srivastava, V.M.L., Jain, S.K., and Misra-Bhattacharya, S. (2004). Macrophages in the development of protective immunity against experimental Brugia malayi infection. Parasitology *129*, 311–323.

Hadas, E., Derda, M., and Wandurska-Nowak, E. (2001). Effect of exogenous nitric oxide in experimental trichinellosis. Parasitol. Res. 86–88.

Hahn, U.K., Bender, R.C., and Bayne, C.J. (2001). Involvement of nitric oxide in killing of Schistosoma mansoni sporocysts by hemocytes from resistant Biomphalaria glabrata. J. Parasitol. *87*, 778–785.

Hamilton, C.M., Brandes, S., Holland, C. V., and Pinelli, E. (2008). Cytokine expression in the brains of Toxocara canis-infected mice. Parasite Immunol. *30*, 181–185.

Hausladen, A., and Fridovich, I. (1994). Superoxide and peroxynitrite inactivate aconitases, but nitric oxide does not. J. Biol. Chem. *269*, 29405–29408.

Hayes, T.J., and Mitrovič, M. (1977). The Early Expression of Protective Immunity to Fasciola hepatica in Rats. J. Immunol. *63*, 584–587.

Hess, D.T., Matsumoto, A., Kim, S., Marshall, H.E., and Stamler, J.S. (2005). Protein S-nitrosylation: purview and parameters. *6*, 150–166.

Hesse, M., Cheever, A.W., Jankovic, D., and Wynn, T.A. (2000). NOS-2 mediates the protective anti-inflammatory and antifibrotic effects of the Th1-inducing adjuvant, IL-12, in a Th2 model of granulomatous disease. Am. J. Pathol. *157*, 945–955.

Hesse, M., Modolell, M., La Flamme, A.C., Schito, M., Fuentes, J.M., Cheever, A.W., Pearce, E.J., and Wynn, T.A. (2001). Differential Regulation of Nitric Oxide Synthase-2 and Arginase-1 by Type 1/Type 2 Cytokines In Vivo: Granulomatous Pathology Is Shaped by the Pattern of L-Arginine Metabolism. J. Immunol. *167*, 6533–6544.

Heuer, L., Beyerbach, M., Lühder, F., Beineke, A., and Strube, C. (2015). Neurotoxocarosis alters myelin protein gene transcription and expression. Parasitol. Res. *114*, 2175–2186.

Hirata, M., Hirata, K., Kage, M., Zhang, M., Hara, T., and Fukuma, T. (2001). Effect of nitric oxide synthase inhibition on Schistosoma japonicum egg-induced granuloma formation in the mouse liver. Parasite Immunol. *23*, 281–289.

Horak, P., Dvorak, J., Kolarova, L., and Trefil, L. (1999). Trichobilharzia regenti, a pathogen of the avian and mammalian central nervous systems. Parasitology *119 (Pt 6*, 577–581.

Howe, S., Zöphel, D., Subbaraman, H., Unger, C., Held, J., Engleitner, T., Hoffmann, W.H., and Kreidenweissa, A. (2015). Lactate as a novel quantitative measure of viability in Schistosoma mansoni drug sensitivity assays. Antimicrob. Agents Chemother. *59*, 1193–1199.

Hrádková, K., and Horák, P. (2002). Neurotropic behaviour of Trichobilharzia regenti in ducks and

mice. J. Helminthol. *76*, 137–142.

Huie, R.E., and Padmaja, S. (1993). The reaction of NO with superoxide. Free Radic. Res. Commun. *18*, 195–199.

James, S.L. (1995). Role of nitric oxide in parasitic infections. Microbiol. Rev. *59*, 533–547.

James, S.L., and Glaven, J. (1989). Macrophage cytotoxicity against schistosomula of Schistosoma mansoni involves arginine-dependent production of reactive nitrogen intermediates. J. Immunol. *143*, 4208–4212.

Jedlina, L., Kozak-Ljunggren, M., and Wedrychowicz, H. (2011). In vivo studies of the early, peritoneal, cellular and free radical response in rats infected with Fasciola hepatica by flow cytometric analysis. Exp. Parasitol. *128*, 291–297.

Juedes, M.J., and Wogan, G.N. (1996). Peroxynitrite-induced mutation spectra of pSP189 following replication in bacteria and in human cells. Mutat. Res. - Fundam. Mol. Mech. Mutagen. *349*, 51–61.

Kanazawa, T., Asahi, H., Hata, H., Mochida, K., Kagei, N., and Stadecker, M.J. (1993). Arginine-dependent generation of reactive nitrogen intermediates is instrumental in the in vitro killing of protoscoleces of Echinococcus multilocularis by activated macrophages. *15*, 619–623.

Kołodziej-Sobocińska, M., Dziemian, E., and Machnicka-Rowińska, B. (2006). Inhibition of nitric oxide production by aminoguanidine influences the number of Trichinella spiralis parasites in infected “low responders” (C57BL/6) and “high responders” (BALB/c) mice. Parasitol. Res. *99*, 194–196.

Kouřilová, P., Hogg, K.G., Kolářová, L., and Mountford, A.P. (2004a). Cercarial dermatitis caused by bird schistosomes comprises both immediate and late phase cutaneous hypersensitivity reactions. J. Immunol. *172*, 3766–3774.

Kouřilová, P., Syrůček, M., and Kolářová, L. (2004b). The severity of mouse pathologies caused by the bird schistosome Trichobilharzia regenti in relation to host immune status. Parasitol. Res. *93*, 8–16.

Krammer, P.H., Kubelka, C.F., Falk, W., and Ruppel, A. (1985). Priming and triggering of tumoricidal and schistosomulicidal macrophages by two sequential lymphokine signals: interferon-γ and macrophage cytotoxicity inducing factor 2. *135*, 3258–3263.

Lawrence, C.E., Paterson, J.C., Wei, X.Q., Liew, F.Y., Garside, P., and Kennedy, M.W. (2000). Nitric oxide mediates intestinal pathology but not immune expulsion during Trichinella spiralis infection

in mice. J. Immunol. *164*, 4229–4234.

Leontovyč, R., Young, N.D., Korhonen, P.K., Hall, R.S., Tan, P., Mikeš, L., Kašný, M., Horák, P., and Gasser, R.B. (2016). Comparative Transcriptomic Exploration Reveals Unique Molecular Adaptations of Neuropathogenic Trichobilharzia to Invade and Parasitize Its Avian Definitive Host. PLoS Negl. Trop. Dis. *10*, 1–24.

Li Hsü, S.Y., Hsü, H.F., Isacson, P., and Cheng, H.F. (1977). Schistosoma mansoni and S . japonicum : Methylene Blue Test for the Viability of Schistosomula in vitro. Exp. Parasitol. *41*, 329–334.

Lichtenbergová, L., Lassmann, H., Jones, M.K., Kolářová, L., and Horák, P. (2011). Trichobilharzia regenti: Host immune response in the pathogenesis of neuroinfection in mice. Exp. Parasitol. *128*, 328–335.

Lin, S.M., Liao, C.W., Lin, Y.H., Lee, C.C., Kao, T.C., and Fan, C.K. (2008). Inducible nitric oxide synthase inhibition influenced granuloma formation with suppressed collagen expression in myositis caused by Toxocara canis in mice. Parasitol. Res. *102*, 577–585.

Liu, J., Pan, T., You, X., Xu, Y., Liang, J., Limpanont, Y., Sun, X., and Okanurak, K. (2015). SjCa8 , a calcium-binding protein from Schistosoma japonicum , inhibits cell migration and suppresses nitric oxide release of RAW264 . 7 macrophages. Parasit. Vectors 1–15.

Lomonosova, E.E., Kirsch, M., Rauen, U., and De Groot, H. (1998). The critical role of Hepes in SIN-1 cytotoxicity, peroxynitrite versus hydrogen peroxide. Free Radic. Biol. Med. *24*, 522–528.

Louveau, A., Plog, B.A., Antila, S., Alitalo, K., Nedergaard, M., and Kipnis, J. (2017). Understanding the functions and relationships of the glymphatic system and meningeal lymphatics. J. Clin. Invest. *127*, 3210–3219.

Macháček, T., Panská, L., Dvořáková, H., and Horák, P. (2016). Nitric oxide and cytokine production by glial cells exposed in vitro to neuropathogenic schistosome Trichobilharzia regenti. Parasit. Vectors *9*, 579.

Madigan, C.A., Cambier, C.J., Kelly-Scumpia, K.M., Scumpia, P.O., Cheng, T.Y., Zailaa, J., Bloom, B.R., Moody, D.B., Smale, S.T., Sagasti, A., et al. (2017). A Macrophage Response to Mycobacterium leprae Phenolic Glycolipid Initiates Nerve Damage in Leprosy. Cell *170*, 973-985.e10.

Majer, M. (2018). Production of cytokines in mice infected with bird schistosome Trichobilharzia regenti. Master's thesis. Charles University.

Marcelo, C., Carvalho, E., Silverio, J.C., Alice, A., Marchevsky, R.S., Xavier, S.S., Gazzinelli, R.T., and

Glo, M. (2012). Inducible Nitric Oxide Synthase in Heart Tissue and Nitric Oxide in Serum of Trypanosoma cruzi-Infected Rhesus Monkeys : Association with Heart Injury. *6*.

McLaren, D.J., and James, S.L. (1985). Ultrastructural studies of the killing of schistosomula of Schistosoma mansoni by activated macrophages in vitro. Parasite Immunol. *7*, 315–331.

Ming, L., Peng, R.Y., Zhang, L., Zhang, C.L., Lv, P., Wang, Z.Q., Cui, J., and Ren, H.J. (2016). Invasion by Trichinella spiralis infective larvae affects the levels of inflammatory cytokines in intestinal epithelial cells in vitro. Exp. Parasitol. *170*, 220–226.

Miranda, M.M., Panis, C., Henrique, A., and Cataneo, D. (2015). Nitric Oxide and Brazilian Propolis Combined Accelerates Tissue Repair by Modulating Cell Migration , Cytokine Production and Collagen Deposition in Experimental Leishmaniasis. 1–19.

Mishra, B.B., Gundra, U.M., and Teale, J.M. (2012). STAT6-/- mice exhibit decreased cells with alternatively activated macrophage phenotypes and enhanced disease severity in murine neurocysticercosis. J. Neuroimmunol. *232*, 26–34.

Mourglia-Ettlin, G., Merlino, A., Capurro, R., and Dematteis, S. (2015). Susceptibility and resistance to Echinococcus granulosus infection: Associations between mouse strains and early peritoneal immune responses. Immunobiology *221*, 418–426.

Negi, N., and Das, B.K. (2018). CNS: Not an immunoprivilaged site anymore but a virtual secondary lymphoid organ. Int. Rev. Immunol. *37*, 57–68.

Nilsson, B.O. (1999). Biological effects of aminoguanidine: An update. Inflamm. Res. *48*, 509–515.

Oswald, I.P., Eltoum, I., Wynn, T.A., Schwartz, B., Caspar, P., Paulin, D., Sher, A., and James, S.L. (1994). Endothelial cells are activated by cytokine treatment to kill an intravascular parasite, Schistosoma mansoni, through the production of nitric oxide. Proc. Natl. Acad. Sci. *91*, 999–1003.

Pacheco, I.L., Abril, N., Bautista, M.J., Zafra, R., Escamilla, A., Ruiz, M.T., and Pérez, J. (2017). Th1/Th2 balance in the liver and hepatic lymph nodes of vaccinated and unvaccinated sheep during acute stages of infection with Fasciola hepatica. Vet. Parasitol. *238*, 61–65.

Pankrác, J., Macháček, T., Kašný, M., Horák, P. (2017). Effect of nitric oxide and hydrogen peroxide on avian schistosome Trichobilharzia regenti and Trichobilharzia szidati. Helminthological days 2017.

Paoliello-Paschoalato, A.B., Oliveira, S.H.P., and Cunha, F.Q. (2005). Interleukin 4 induces the expression of inducible nitric oxide synthase in eosinophils. Cytokine *30*, 116–124.

Pérez-Caballero, R., Buffoni, L., Martínez-Moreno, F.J., Zafra, R., Molina-Hernández, V., Pérez, J., and Martínez-Moreno, Á. (2018). Expression of free radicals by peritoneal cells of sheep during the early stages of Fasciola hepatica infection. Parasit. Vectors 1–11.

Piedrafita, D., Parsons, J.C., Sandeman, R.M., Wood, P.R., Estuningsih, S.E., Partoutomo, S., and Spithill, T.W. (2001). Antibody-dependent cell-mediated cytotoxicity to newly excysted juvenile Fasciola hepatica in vitro is mediated by reactive nitrogen intermediates. Parasite Immunol. *23*, 473–482.

Rabelo, L.A., Todiras, M., Nunes-souza, V., and Qadri, F. (2016). Genetic Deletion of ACE2 Induces Vascular Dysfunction in C57BL / 6 Mice : Role of Nitric Oxide Imbalance and Oxidative Stress. 1–16.

Rajan, T. V., Porte, P., Yates, J.A., Keeper, L., and Shultz, L.D. (1996). Role of nitric oxide in host defense against an extracellular, metazoan parasite, Brugia malayi. Infect. Immun. *64*, 3351–3353.

Ramaswamy, K., He, Y.X., and Salafsky, B. (1997). ICAM-1 and iNOS expression increased in the skin of mice after vaccination with γ-irradiated cercariae of Schistosoma mansoni. Exp. Parasitol. *86*, 118–132.

Rew, R.S., and Saz, H.J. (1977). The carbohydrate metabolism of Brugia pahangi microfilariae. J. Parasitol. *63*, 123–129.

Rodrigues, R.M., Lúcia, A., Gonçalves, R., Maria, N., Ribeiro, C., Cardoso, D.B., Rodrigues, N., Loyane, A., Ronaldo, C., Marlene, A., et al. (2018). Inducible nitric oxide synthase controls experimental Strongyloides infection. 1–9.

Rodríguez-Sosa, M., Saavedra, R., Tenorio, E.P., Rosas, L.E., Satoskar, A.R., and Terrazas, L.I. (2004). A STAT4-dependent Th1 response is required for resistance to the helminth parasite Taenia crassiceps. Infect. Immun. *72*, 4552–4560.

Rojas-Caraballo, J., López-Abán, J., Moreno-Pérez, D.A., Vicente, B., Fernández-Soto, P., del Olmo, E., Patarroyo, M.A., and Muro, A. (2017). Transcriptome profiling of gene expression during immunisation trial against Fasciola hepatica: identification of genes and pathways involved in conferring immunoprotection in a murine model. BMC Infect. Dis. *17*, 94.

Romero-Puertas, M.C., Campostrini, N., and Mattè, A. (2008). Proteomic analysis of S-nitrosylated proteins in Arabidopsis thaliana undergoing hypersensitive response. 1459–1469.

Ruano, A.L., López-Abán, J., Gajate, C., Mollinedo, F., De Melo, A.L., and Muro, A. (2012). Apoptotic mechanisms are involved in the death of Strongyloides venezuelensis after triggering of nitric oxide. Parasite Immunol. *34*, 570–580.

Ruano, A.L., López-Abán, J., Fernández-Soto, P., De Melo, A.L., and Muro, A. (2015). Treatment with nitric oxide donors diminishes hyperinfection by Strongyloides venezuelensis in mice treated with dexamethasone. Acta Trop. *152*, 90–95.

Sadeghi-Hashjin, G., and Naem, S. (2001). Parasiticidal effects of peroxynitrite on ovine liver flukes in vitro. J. Helminthol. *75*, 73–76.

Samant, M., Gupta, R., Kumari, S., Misra, P., Khare, P., Kushawaha, P.K., Sahasrabuddhe, A.A., and Dube, A. (2009). Immunization with the DNA-Encoding N-Terminal Domain of Proteophosphoglycan of Leishmania donovani Generates Th1-Type Immunoprotective Response against Experimental Visceral Leishmaniasis . J. Immunol. *183*, 470–479.

Shaw, M.K., and Erasmus, D.A. (1987). Schistosoma mansoni: Structural damage and tegumental repair after in vivo treatment with praziquantel. Parasitology *94*, 243–254.

Shen, J., Lai, D.-H., Wilson, R.A., Chen, Y.-F., Wang, L.-F., Yu, Z.-L., Li, M.-Y., He, P., Hide, G., Sun, X., et al. (2017). Nitric oxide blocks the development of the human parasite *Schistosoma japonicum*. Proc. Natl. Acad. Sci. 201708578.

Sher, A., James, S.L., Simpson, A.J., Lazdins, J.K., and Meltzer, M.S. (1982). Macrophages as effector cells of protective immunity in murine schistosomiasis. III. Loss of susceptibility to macrophage-mediated killing during maturation of S. mansoni schistosomula from the skin to the lung stage. J. Immunol. (Baltimore, Md. 1950) *128*, 1876–1879.

Shi, S.R., Cote, R.J., and Taylor, C.R. (1997). Antigen retrieval immunohistochemistry: Past, present, and future. J. Histochem. Cytochem. *45*, 327–343.

Shrager, P., and Youngman, M. (2017). Preferential conduction block of myelinated axons by nitric oxide. J. Neurosci. Res. *95*, 1402–1414.

Shultz, R.B., and Zhong, Y. (2017). Minocycline targets multiple secondary injury mechanisms in traumatic spinal cord injury. Neural Regen. Res. *12*, 702–713.

Sibille, P., Tliba, O., and Boulard, C. (2004). Early and transient cytotoxic response of peritoneal cells from Fasciola hepatica-infected rats. Vet. Res. *33*, 573–584.

Simmons, M.L., and Murphy, S. (1992). Induction of Nitric Oxide Synthase in Glial Cells.

Sirsjö, A., Karlsson, M., Gidlöf, A., Rollman, O., and Törmä, H. (1996). Increased expression of inducible nitric oxide synthase in psoriatic skin and cytokine-stimulated cultured keratinocytes. Br. J. Dermatol. *134*, 643–648.

Springer, A., Heuer, L., Janecek-erfurth, E., Beineke, A., and Strube, C. (2019). Histopathological characterization of Toxocara canis - and T . cati -induced neurotoxocarosis in the mouse model.

Steers, N.J.R., Rogan, M.T., and Heath, S. (2001). In-vitro susceptibility of hydatid cysts of Echinococcus granulosus to nitric oxide and the effect of the laminated layer on nitric oxide production. Parasite Immunol. *23*, 411–417.

Stewart, V.C., Heslegrave, A.J., Brown, G.C., Clark, J.B., and Heales, S.J.R. (2002). Nitric oxide-dependent damage to neuronal mitochondria involves the NMDA receptor. Eur. J. Neurosci. *15*, 458–464.

Stuehr, D.J., and Marletta, M. a (1985). Mammalian nitrate biosynthesis: mouse macrophages produce nitrite and nitrate in response to Escherichia coli lipopolysaccharide. Proc. Natl. Acad. Sci. U. S. A. *82*, 7738–7742.

Stuehr, D.J., Gross, S.S., Sakuma, I., Levi, R., and Nathan, C.F. (1989). Activated murine macrophages secrete a metabolite of arginine with the bioactivity of endothelium-derived relaxing factor and the chemical reactivity of nitric oxide. J. Exp. Med. *169*, 1011–1020.

Taylor, M.J., Cross, H.F., Mohammed, A.A., Trees, A.J., and Bianco, A.E. (1996). Susceptibility of Brugia malayi and Onchocerca lienalis microfilariae to nitric oxide and hydrogen peroxide in cell-free culture and from IFNy-activated macrophages. Parasitology *112*, 315–322.

Terrazas, L.I., Cruz, M., Rodríguez-Sosa, M., Bojalil, R., García-Tamayo, F., and Larralde, C. (1999). Th1-type cytokines improve resistance to murine cysticercosis caused by Taenia crassiceps. Parasitol. Res. *85*, 135–141.

Thomas, G.R., McCrossan, M., and Selkirk, M.E. (1997). Cytostatic and cytotoxic effects of activated macrophages and nitric oxide donors on Brugia malayi. Infect. Immun. *65*, 2732–2739.

Thomas, P.G., Carter, M.R., Atochina, O., Da'Dara, A.A., Piskorska, D., McGuire, E., and Harn, D.A. (2003). Maturation of Dendritic Cell 2 Phenotype by a Helminth Glycan Uses a Toll-Like Receptor 4-Dependent Mechanism. J. Immunol. *171*, 5837–5841.

Tracey, W.R., Tse, J., and Carter, G. (1995). Lipopolysaccharide-Induced Changes in Plasma Nitrite and Nitrate Concentrations in Rats and Mice: Pharmacological Evaluation of Nitric Oxide Synthase Inhibitors. J. Pharmacol. Exp. Ther. 1011–1015.

Tsikas, D., and Duncan, M.W. (2014). Mass spectrometry and 3-nitrotyrosine: strategies, controversies, and our current perspective. Mass Spectrom. Rev. 237–276.

Venkataramana, S., Lourenssen, S., Miller, K.G., and Blennerhassett, M.G. (2015). Early inflammatory damage to intestinal neurons occurs via inducible nitric oxide synthase. Neurobiol. Dis. *75*, 40–52.

Verma, S.K., Joseph, S.K., Verma, R., Kushwaha, V., Parmar, N., Yadav, P.K., Thota, J.R., Kar, S., and Murthy, P.K. (2015). Protection against filarial infection by 45-49 kDa molecules of Brugia malayi via IFN-γ-mediated iNOS induction. Vaccine *33*, 527–534.

Vernia, S., Sanz-González, S.M., and López-García, M.P. (2001). Involvement of peroxynitrite on the early loss of P450 in short-term hepatocyte cultures. In Biological Reactive Intermediates VI: Chemical and Biological Mechanisms in Susceptibility to and Prevention of Environmental Diseases, P.M. Dansette, R. Snyder, M. Delaforge, G.G. Gibson, H. Greim, D.J. Jollow, T.J. Monks, and I.G. Sipes, eds. (Boston, MA: Springer US), pp. 209–212.

Vrbová, K. (2017). In vitro cultivation of the trematode species Trichobilharzia regenti. Master's Thesis. Charles University.

Wade, R.S., and Castro, C.E. (1990). Redox reactivity of iron(III) porphyrins and heme proteins with nitric oxide. Nitrosyl transfer to carbon, oxygen, nitrogen and sulfur. Chem. Res. Toxicol. *3*, 289–291.

Wisastra, R., Poelstra, K., Bischoff, R., Maarsingh, H., Haisma, H.J., and Dekker, F.J. (2011). Antibody-free detection of protein tyrosine nitration in tissue sections. ChemBioChem *12*, 2016–2020.

Wynn, T.A., Oswald, I.P., Eltoum, I.A., Caspar, P., Lowenstein, C.J., Lewis, F.A., James, S.L., and Sher, A. (1994). Elevated Expression of Th1 Cytokines and Nitric-Oxide Synthase in the Lungs of Vaccinated Mice after Challenge Infection with Schistosoma-Mansoni. J. Immunol. *153*, 5200–5209.

Yang, Q., Shen, J., Jiang, Z., Shi, Y., Wan, X., and Yang, Y. (2017). TLR2 signal influences the iNOS / NO responses and worm development in C57BL / 6J mice infected with Clonorchis sinensis. 1–10.

Zafra, R., Pérez-Écija, R.A., Buffoni, L., Moreno, P., Bautista, M.J., Martínez-Moreno, A., Mulcahy, G., Dalton, J.P., and Pérez, J. (2013). Early and Late Peritoneal and Hepatic Changes in Goats Immunized with Recombinant Cathepsin L1 and Infected with Fasciola hepatica. J. Comp. Pathol. *148*, 373–384.

Zhang, N., Diao, Y., Hua, R., Wang, J., Han, S., Li, J., and Yin, Y. (2017). Nitric oxide-mediated pathways and its role in the degenerative diseases 2 . 2 . Effects of NO on major disease-related biological processes 2 . 1 . The synthesis and functions of nitric oxide in the physiological conditions. 824–834.

Zheng, Y. (2013). International Immunopharmacology Strategies of Echinococcus species responses to immune attacks : Implications for therapeutic tool development. Int. Immunopharmacol. *17*, 495–501.

Zheng, Y., Guo, X., He, W., Shao, Z., Zhang, X., Yang, J., Shen, Y., Luo, X., and Cao, J. (2016). International Immunopharmacology Effects of Echinococcus multilocularis miR-71 mimics on murine. Int. Immunopharmacol. *34*, 259–262.

Zheng, Y., Guo, X., Su, M., Guo, A., Ding, J., and Yang, J. (2017). Veterinary Parasitology Regulatory effects of Echinococcus multilocularis extracellular vesicles. Vet. Parasitol. *235*, 29–36.

Supplementary data

Supplement 1: Signal colocalization

Colocalization of 3-NT and DAPI signals was examined in the spinal cord of mice 7 dpi using confocal microscopy. Even though the signals were seemingly in one spot (see Figure S1A), they are rather next to each other than overlapping suggesting that 3-NT formed in close proximity to nuclei but not directly on nuclear lamina.

Additionally, colocalization of iNOS and Iba-1/GFAP signals was also examined in the spinal cord of mice 3 dpi using confocal microscopy. However, the colocalization of iNOS and the glial cell markers was not observed (see Figure S1B, C) suggesting that neither microglia nor astrocytes were the cells responsible for NO production in the infected tissue.

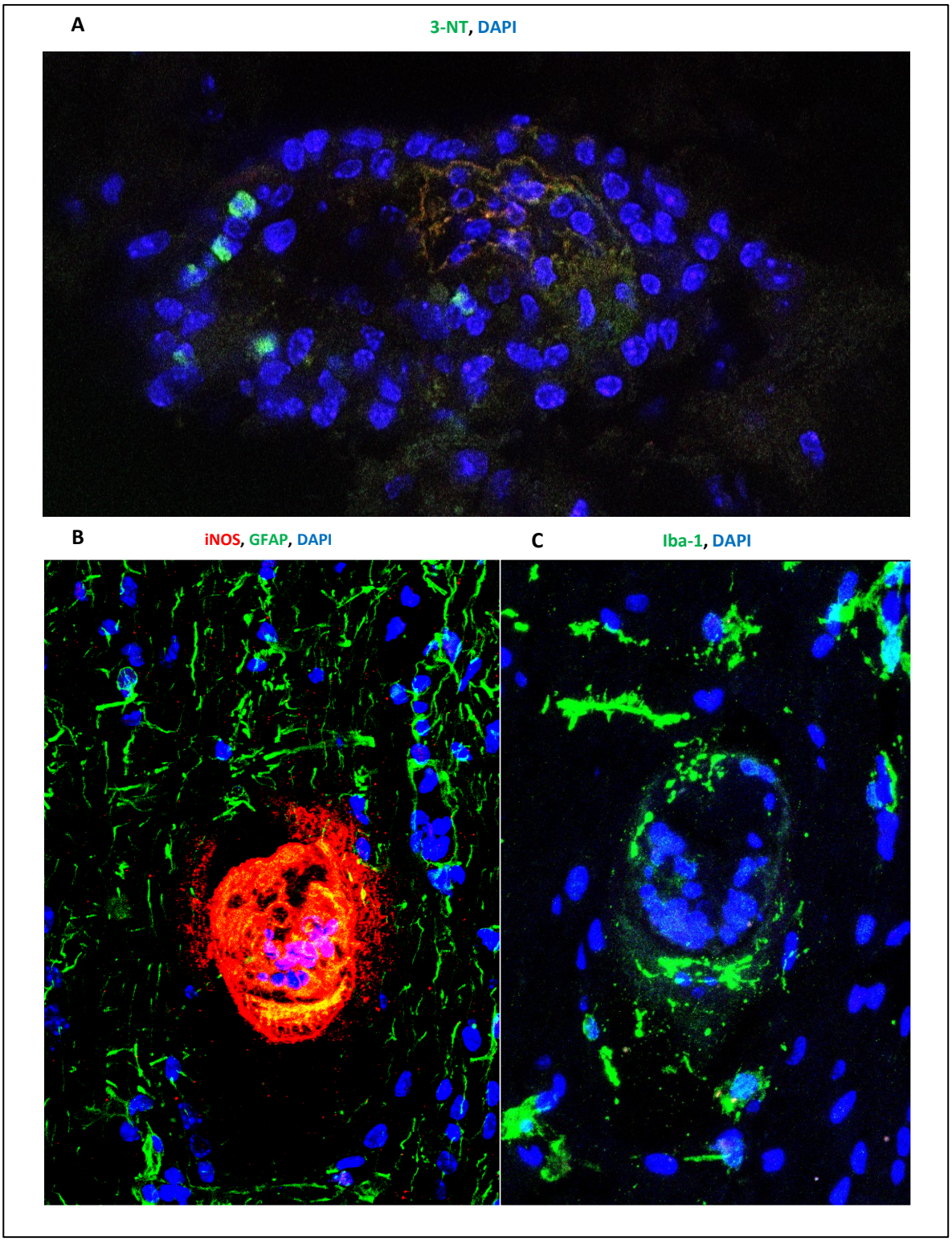

Figure S1: A: *Colocalization of 3-NT (green) signal with DAPI (blue).* B, C: *Colocalization of iNOS (red) signal with GFAP (marker of astrocytes, green) and DAPI (blue) (B) and subsequent lamina of spinal cord with marked Iba-1 (marker of microglia, green) and DAPI (blue) (C).*

Supplement 2: Nitrite/nitrate levels in sera after AG treatment

Nitrite/nitrate levels in sera measured using Griess reaction show NO levels on a systemic level. This minor experiment served as a control of NO production in mice included in experiment testing the AG effect on *T. regenti* infection in mice. The trend observed in Figure S1 is very similar to the trend shown in Figure 2.

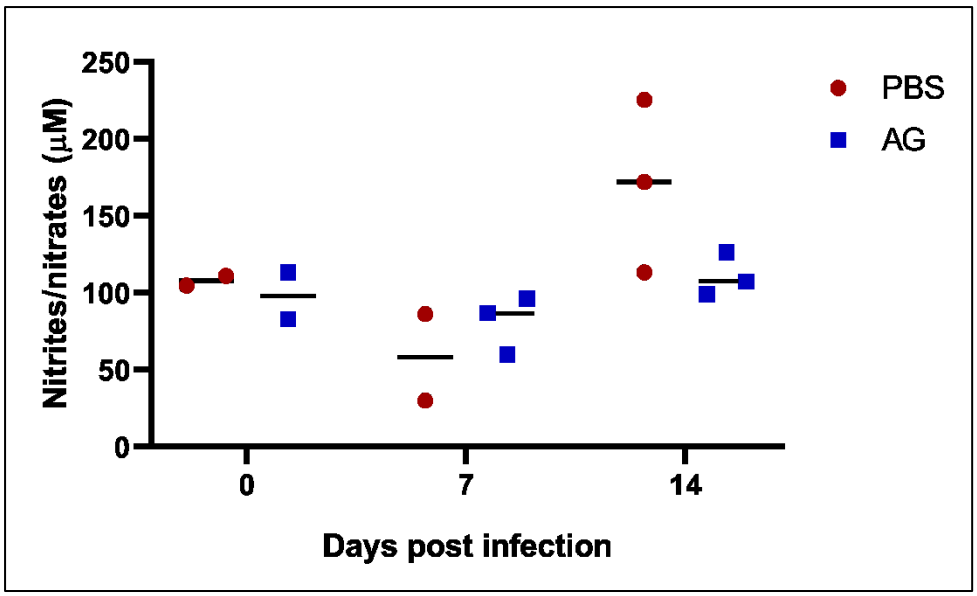

Figure S2: Nitrite/nitrate levels measured by Griess reaction in sera obtained from T. regenti *infected mice with AG injections (blue) and control PBS (red) injections at 0, 7 and 14 days post infection.*

Supplement 3: Parasite burden after AG treatment

After NO production impairment by AG-treatment, schistosomula burden was established in segments of spinal cord (cervical, thoracic, lumbar and sacral) and areas of spinal cord (grey matter, white matter, border of grey and white matter, submeningeal area). This analysis was performed only on subset of schistosomula-positive slides that were stained for MBP. Table S1 shows the detailed overview of parasite burden with respect both to spinal cord segment and localization, summary data are presented in Table 9.

Table S1: Summary of parasite burden in both segments and areas of spinal cord at 7 and 14 dpi with AG and PBS injections. Abbreviations: dpi – days post infection; gm – grey matter; wm – white matter; gm/wm – border of white and grey matter; sm – submeningeal area.

Spinal cord segment	**Area**	**No. of stained schistosomula**			
		7 dpi		**14 dpi**	
		PBS	**AG**	**PBS**	**AG**
Cervical	**gm**	0	0	0	1
	wm	0	1	2	1
	gm/wm	2	0	1	0
	sm	0	0	1	0
Thoracic	**gm**	1	0	0	1
	wm	5	3	5	3
	gm/wm	0	1	3	0
	sm	0	1	1	4
Lumbar	**gm**	0	0	0	0
	wm	1	1	2	3
	gm/wm	0	1	0	0
	sm	0	1	0	1